


Isolation and characterization of fast-growing green snow bacteria from coastal East Antarctica

Margarita Smirnova¹  | Uladzislau Miamin² | Achim Kohler¹ | Leonid Valentovich^{2,3} | Artur Akhremchuk³ | Anastasiya Sidarenka^{2,3} | Andrey Dolgikh⁴ | Volha Shapaval¹

¹Faculty of Science and Technology, Norwegian University of Life Sciences, Ås, Norway

²Faculty of Biology, Belarusian State University, Minsk, Belarus

³Institute of Microbiology, National Academy of Sciences of Belarus, Minsk, Belarus

⁴Institute of Geography, Russian Academy of Sciences, Moscow, Russia

Correspondence

Margarita Smirnova, Faculty of Science and Technology, Norwegian University of Life Sciences, Postbox 5003, 1432 Ås, Norway.

Email: margarita.smirnova@nmbu.no

Funding information

Eurasia program, SIU, Grant/Award Number: CPEA-LT-2016/10126

Abstract

Snow microorganisms play a significant role in climate change and affecting the snow melting rate in the Arctic and Antarctic regions. While research on algae inhabiting green and red snow has been performed extensively, bacteria dwelling in this biotope have been studied to a much lesser extent. In this study, we performed 16S rRNA gene amplicon sequencing of two green snow samples collected from the coastal area of the eastern part of Antarctica and conducted genotypic and phenotypic profiling of 45 fast-growing bacteria isolated from these samples. 16S rRNA gene amplicon sequencing of two green snow samples showed that bacteria inhabiting these samples are mostly represented by families *Burkholderiaceae* (46.31%), *Flavobacteriaceae* (22.98%), and *Pseudomonadaceae* (17.66%). Identification of 45 fast-growing bacteria isolated from green snow was performed using 16S rRNA gene sequencing. We demonstrated that they belong to the phyla *Actinobacteria* and *Proteobacteria*, and are represented by the genera *Arthrobacter*, *Cryobacterium*, *Leifsonia*, *Salinibacterium*, *Paeniglutamicibacter*, *Rhodococcus*, *Polaromonas*, *Pseudomonas*, and *Psychrobacter*. Nearly all bacterial isolates exhibited various growth temperatures from 4°C to 25°C, and some isolates were characterized by a high level of enzymatic activity. Phenotyping using Fourier transform infrared (FTIR) spectroscopy revealed a possible accumulation of intracellular polymer polyhydroxyalkanoates (PHA) or lipids in some isolates. The bacteria showed different lipids/PHA and protein profiles. It was shown that lipid/PHA and protein spectral regions are the most discriminative for differentiating the isolates.

KEYWORDS

16S rRNA gene amplicon sequencing, 16S rRNA gene sequencing, Antarctic bacteria, Fourier transform infrared (FTIR) spectroscopy, green snow, principal component analysis

1 | INTRODUCTION

Snow cover in the Arctic and Antarctic regions is critically important for regulating the Earth's climate and biogeochemical cycles (Maccario

et al., 2019). The largest proportion of the glacial surfaces in the Arctic and Antarctic is covered by snow, where permanent and seasonal snow can account for up to 35% of the entire Earth's surface (Lutz et al., 2016). Snow is a physically, chemically, and biologically dynamic

This is an open access article under the terms of the Creative Commons Attribution-NonCommercial-NoDerivs License, which permits use and distribution in any medium, provided the original work is properly cited, the use is non-commercial and no modifications or adaptations are made.

© 2020 The Authors. *MicrobiologyOpen* published by John Wiley & Sons Ltd.

ecosystem having a connection to the atmosphere above and to the soil or ice below (Malard et al., 2019). The microbial content of snow ranges from 10^3 to 10^4 cells per ml of melted snow (Maccario et al., 2015). Snow microorganisms are exposed to a range of specific physicochemical conditions—different levels of UV radiation at the surface, low water activity, extremely low temperatures, and limited oligotrophic nutrient conditions (Maccario et al., 2019; Malard et al., 2019), and therefore, they can exhibit biotechnologically interesting properties. In the last decade, the biotechnological and ecological properties of snow microorganisms have attracted attention, and a large number of studies on the isolation, identification, and genotypic and phenotypic characterization of various snow microorganisms have been conducted worldwide (Frey et al., 2013; Klassen & Foght, 2011; Kojima et al., 2009; Larose et al., 2013; Maccario et al., 2014; Maki et al., 2011; Margesin & Miteva, 2011; Zeng et al., 2013). It has been reported that the number and diversity of snow microbiota vary depending on location, season, and depth (Carpenter et al., 2000; Chuvochina et al., 2011; Harding et al., 2011; Larose et al., 2010; Lazzaro et al., 2015; Lopatina et al., 2013; Maccario et al., 2014, 2019; Michaud et al., 2014; Møller et al., 2013; Wunderlin et al., 2016; Zhang et al., 2010).

Arctic and Antarctic regions start to be significantly affected by global warming, which is leading to a rapid increase in glacial snowmelt in both areas. Recently, it was reported that snow microorganisms can contribute to an increase in the snow melting rate (Lutz et al., 2016). Also, it has been shown that snow algae are one of the critical players in glacial snow melting and the dominant microbial community in the melted snow (Lutz et al., 2014, 2016). Algae are the primary colonizers of melted snow, and they form extensive snow blooms in spring and summer (Lutz et al., 2016). Algal snow blooms are coloring the melted snow in red or green colors because of their red or green pigments, which are produced as a result of either photosynthesis or protection from different environmental stress conditions, for example, a high level of UV radiation (Fujii et al., 2010). Such snow blooming phenomenon is called “red” and “green” snow. Currently, several scientific reports are published on algae isolated from the red and green snow (Akiyama, 1979; Ling & Seppelt, 1993; Milius, 2000; Thomas & Duval, 1995), while little attention has been given to the bacterial communities associated with those algae. For example, it was shown that most bacteria isolated from the colored snow belong to phyla *Proteobacteria* and *Bacteroidetes* (Davey et al., 2019; Terashima et al., 2017). Besides, the amplicon-sequencing studies of colored snow done by Hisakawa et al. and Terashima et al. revealed algae from genera *Chloromonas*, *Chlamydomonas*, and family *Chrysophyceae* and other eukaryotic microorganisms belonging to phyla *Basidiomycota*, *Cercozoa*, and *Chytridiomycota* (Terashima et al., 2017). The amplicon sequencing of microbial community derived from the non-colored snow and glacier revealed eukaryotic microorganisms such as filamentous fungi from phyla *Ascomycota* and *Basidiomycota* and bacteria from phyla *Proteobacteria*, *Actinobacteria*, and *Firmicutes* (Antony et al., 2016; Baeza et al., 2017; Hisakawa et al., 2015; Lopatina et al., 2013; Sjöling & Cowan, 2003).

In this study, we performed an amplicon sequencing of 16S rRNA genes of two green snow samples obtained from the coastal area of the Eastern part of Antarctica, and a comprehensive genotypic and

phenotypic characterization of 45 fast-growing bacterial isolates obtained from these samples. The characterization was done using traditional and modern analytical technologies: (1) 16S rRNA gene sequencing to determine phylogenetic relationships; (2) microscopy to study cell morphology; (3) enzymatic assays for detecting enzymatic activity; and (4) Fourier transform infrared (FTIR) spectroscopy to study the total cellular biochemical profile. In this study, we apply, for the first time, FTIR spectroscopy for the biochemical fingerprinting of Antarctic fast-growing bacteria. FTIR spectroscopy is a non-destructive next-generation phenotyping technique allowing examining the total biochemical profile of intracellular metabolites in microbial cells by using a high-throughput screening (HTS) measurement mode. Since the early 90s, FTIR spectroscopy has been used for rapid identification and classification of microorganisms in the food and pharmaceutical industry (Van de Voort, 1992; Roggo et al., 2007; Shapaval et al., 2010; Shapaval et al., 2012; Shapaval et al., 2013; Lohumi et al., 2015; Shapaval et al., 2017), for epidemiological investigations in medicine (Amiali et al., 2007; Essendoubi et al., 2007; Colabella et al., 2017), for high-throughput screenings of microbial cell factories (Curk et al., 1994; Shapaval et al., 2014; Kohler et al., 2015; Li et al., 2016; Kosa et al., 2017a, Kosa et al., 2017b, Marova et al., 2017, Kosa et al., 2018b, Shapaval et al., 2019, Xiong et al., 2019a, Xiong et al., 2019b) and biotechnological applications (Naumann, 2000; Harz et al., 2009). Currently, FTIR spectroscopy is extensively used as a next-generation phenotyping method in applied microbiology for the identification, discrimination, and characterization of different microorganisms (Lin et al., 2005; Al-Qadiri et al., 2006; Harz et al., 2009; Shapaval et al., 2010; Amamcharla et al., 2010; Kiefer et al., 2010; Shapaval et al., 2012; Shapaval et al., 2013; Shapaval et al., 2014; Grewal et al., 2014; Kohler et al., 2015; Cámara-Martos et al., 2015; Shapaval et al., 2017; Forfang et al., 2017; Kosa et al., 2017a, Colabella et al., 2017, Kosa et al., 2017b, Kosa et al., 2018b, Shapaval et al., 2019, Dzurendova et al., 2020a). In this study, we utilized FTIR spectroscopy combined with a high-throughput micro-cultivation system (Duetz-MTPS), recently developed by our group (Shapaval et al., 2010, Kosa et al., 2017a, Kosa et al., 2018a, Dzurendova et al., 2020a) allowed performing high-throughput biochemical phenotyping of the isolated green snow Antarctic bacteria grown on agar and broth media. For the FTIR analysis, green snow bacteria were cultivated on both BHI agar and broth media to obtain a complete cellular biochemical profile and to investigate if that profile was affected by the form of the cultivation medium. To study the differences in the biochemical profile of the Antarctic green snow bacteria, visual inspection of the spectra was performed first and then multivariate analysis was applied.

2 | MATERIALS AND METHODS

2.1 | Sampling sites and sampling procedure

Green snow samples (G.S.S) were collected during the 7th Belarusian Antarctic Expedition (2014–2015) from two sites in the Vecherniy District of the Tala Hills oasis, located in the Western

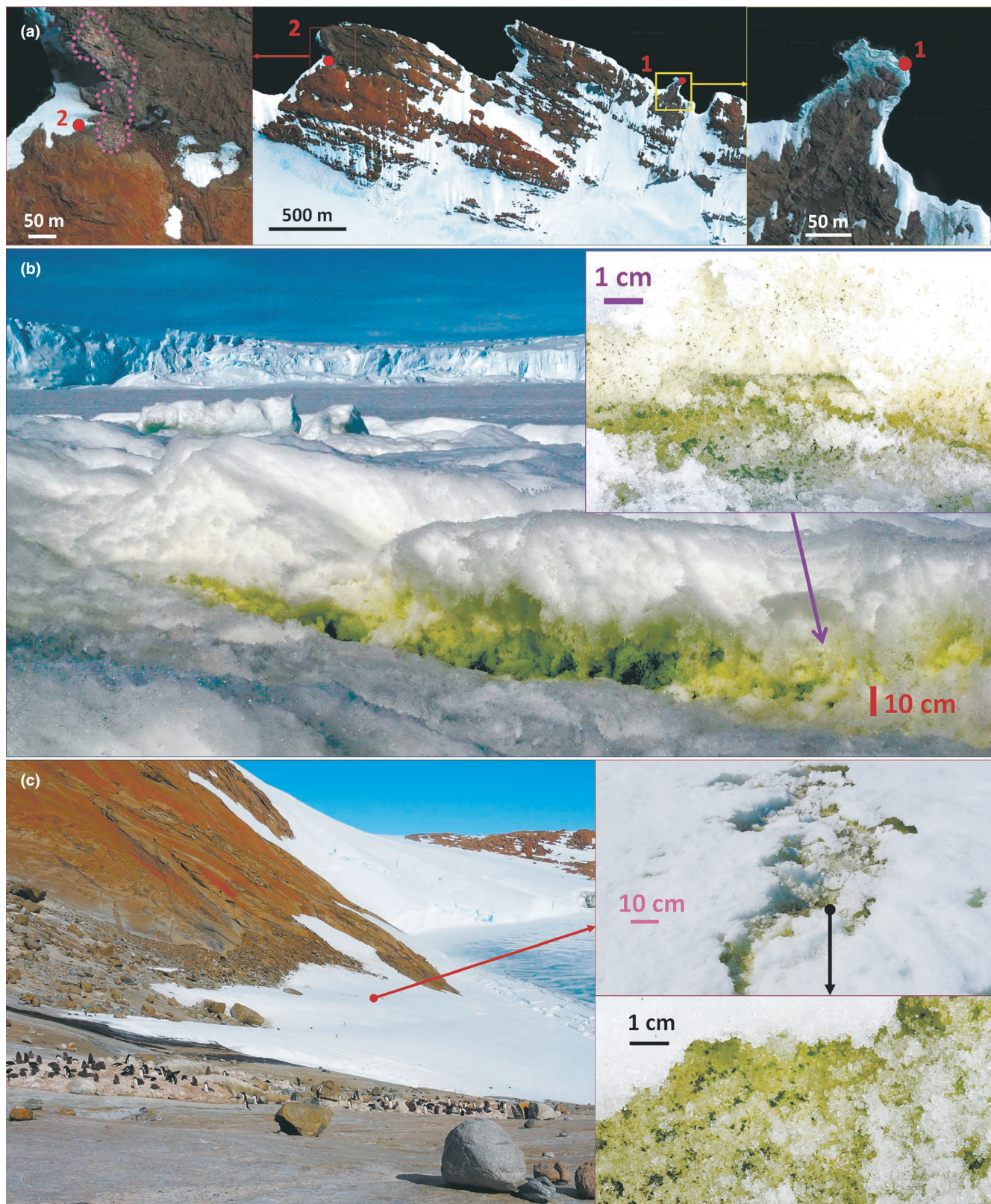


FIGURE 1 Antarctic surface green snow sampling sites: (a) the location on the map; (b) sampling site for the green snow sample 1 (G.S.S1); (c) sampling site for the green snow sample 2 (G.S.S2)

part of Enderby Land (East Antarctica), Mid-Antarctic snow-patch cryptogamic barrens (Bockheim, 2015): G.S.S1 -67.655799 , 46.176633 , 2 m above the sea, 10 meters to the coastline; G.S.S2

-67.65466667 , 46.1072 , 47 m above the sea, 250 m to the coastline, 300 m to the Adelie penguin colony, on a distance of 24 km from the Molodezhnaya station of the Russian Antarctic

Expedition (Figure 1). Samples were taken aseptically into sterile polypropylene tubes with a volume of 50 ml.

2.2 | Determining the number of bacteria in green snow samples

To determine the number of bacteria in green snow samples, epifluorescence microscopy equipped with nuclear filters with a pore diameter of 0.2 μm was used. An Axiovert 25 inverted phase-contrast fluorescence culture microscope with an AxioCam MRc camera (Zeiss, Switzerland) was used for visualization. Prepared green snow samples on glass slides were examined under the immersion lens (100 \times). Processing of the obtained images was conducted in the Image-Pro Plus program.

2.3 | Amplicon sequencing of 16S rRNA genes of green snow samples

2.3.1 | Extraction of total DNA for amplicon sequencing of 16S rRNA genes

Samples of green snow were melted at 4°C, and total cell mass was obtained by centrifugation of 10 ml of melted snow at 15,000 rpm for 15 min. For extracting total genomic DNA, the Genomic DNA Purification Kit (Fermentas, Thermo Fisher Scientific) was used according to the instructions of the manufacturer. The DNA concentration of the DNA green snow extracts was measured fluorometrically with the Qubit dsDNA HS assay kit (Invitrogen), and the extracted DNA was stored at -20°C. Libraries for the sequencing (targeting V3–V4 regions of the 16S rRNA genes) were prepared according to Illumina's "16S Metagenomic Sequencing Library Preparation" guide (https://support.illumina.com/documents/documentation/chemistry_documentation/16s/16s-metagenomic-library-prep-guide-15044223-b.pdf; Part #15044223 Rev. B) with a forward primer: 5' TCGTCGGCAGCGTCA GATGTGTATAAGAGACAGCCTACGGGNGGCWGCAG, and a reverse primer: 5' GTCTCGTGGGCTCGGAGATGTGTATAAGAGACAG GACTACHVGGGTATCTAATCC (Klindworth et al., 2013). Underlining parts in the primers are the locus-specific sites allowing adding index sequences to identify the samples from each other. The integrity of the amplicons was checked by applying electrophoresis with 0.8% agarose gel dipped into the TAE buffer and subsequently stained with ethidium bromide. Molecular weight markers Fermentas SM0311 and SM0321 were used for the determination of replicon size. For the amplicon PCR, a mixture of microbial DNA (5 ng/ μl)—2.5 μl , amplicon PCR forward primer (1 μM)—5 μl , amplicon PCR reverse primer (1 μM)—5 μl , 2 \times KAPA HiFi HotStart Ready Mix—12.5 μl —was used. For performing PCR, the following setup was used: 95°C for 3 min; 25 cycles of 95°C for 30 s, 55°C for 30 s, and 72°C for 30 s; 72°C for 5 min; and hold at 4°C. The PCR products obtained were in the size of ~550 bp. In the

next step, a PCR clean-up 1 was done to purify 16S V3 and V4 amplicons from free primers and primer-dimer species. Further, the index PCR step attaching dual indices and Illumina adapters using the Nextera XT Index 2 Primers (FC-131-1002, Illumina) was performed using the following setup: 95°C for 3 min; 8 cycles of 95°C for 30 s, 55°C for 30 s, and 72°C for 30 s; and 72°C for 5 min. New PCR products with the size of ~630 bp were obtained. In the final step PCR clean-up, 2 AMPure XP beads were used to clean up the final library before quantification. The DNA libraries were quantified using the fluorometric quantification method. The libraries were denatured with NaOH, diluted in the hybridization buffer, and then heat-denatured before MiSeq sequencing. The DNA libraries were sequenced at the Belarusian Research Center for Pediatric Oncology, Hematology and Immunology (Minsk, Belarus) with a MiSeq platform (Illumina, USA) using a MiSeq reagent kit v3 (2 \times 300 bp) and MiSeq paired-end read cell of 300 bp each.

2.3.2 | Analysis of amplicon sequences of 16S rRNA genes

For the analysis of the 16S rRNA gene amplicon sequencing data, the following workflow was used: (1) preprocessing by reads filtering, stitching, and quality control, (2) sequence classification (i.e., identification of the operational taxonomic units), and (3) post-processing by the re-estimation of abundance. The preprocessing of the amplicon sequences of 16S rRNA gene data started from stitching the paired-end reads together using software preprocess16S.py (<https://github.com/masikol/preprocess16S>) where we used an in-house script designed to preprocess reads from regions of 16S rRNA gene. The script allows cutting the amplification primers from the reads. Quality control was performed afterward with kraken2 (Wood et al., 2019). It detects and removes reads that come from other samples, relying on the information whether there are PCR primer sequences in these reads or not. The read merging module merges reads by finding overlapping regions using a naive algorithm: it takes the tail of the forward read and slides it through the reverse read until it finds a significant similarity, where the minimum overlap (20 nt) was used (Gaspar, 2018). If reads are considered as non-overlapping, the algorithm searches for a reference in the Silva database (Quast et al., 2012), and the reference most similar to forward reads was chosen. Then, the algorithm aligns the reverse read against the reference. The algorithm has the following steps:

1. If multiple reference sequences have equal (and the highest) bit score, the script also searches for the best hit for reverse read;
2. If there is a single best-hit reference for both forward and reverse read, the algorithm will choose this reference;
3. If there are multiple best-hit references for forward and reverse reads, the algorithm will choose a reference, which corresponds to the alignment with the minimum number of gaps;

4. If there are multiple references with an equal number of gaps, the algorithm will choose reference with lexicographically the “smallest” accession number in the same way as BLAST does;
5. If forward and reverse reads share no best-hit references, the algorithm retrieves all best-hit references of a forward read from the database and then aligns reverse read against them, choosing the best hit. Again, if the reverse read has multiple best hits, the algorithm chooses one with a minimum number of gaps. And again, if the result is ambiguous, the algorithm will choose a reference with lexicographically the “smallest” accession number.

If forward and reverse reads aligned with a gap, this gap is filled with Ns. The number of allowed Ns was a user-defined value and equal to 35—the length of consensus bacterial conservative region between V3 and V4 hypervariable regions where the Ns are inserted (Whipps, 2001). Taxonomic profiling was performed using the kraken2 (Wood et al., 2019), bracken (Lu et al., 2017) with the default parameters, and precomputed database Silva SSU NR99 (Quast et al., 2012). The output of the pipeline was a set of tables containing the OTU abundances per sample at each level (Table S1 and S2; <https://doi.org/10.5281/zenodo.4297982>).

2.4 | Isolation, identification, and phenotyping of fast-growing green snow bacteria

2.4.1 | Isolation of the fast-growing bacteria from Antarctic green snow

Green snow samples were kept at 4°C until the complete melting of the snow. Then, 0.1 ml of each sample was inoculated on the surface of the meat peptone agar (MPA) (g/L: peptone—5.0; meat extract—1.5; yeast extract—1.5; NaCl—5.0; agar—20.0; pH 7.0 ± 0.2) and cultivated for 10 days at temperatures 5°C and 18°C. A cultivation time of 10 days was chosen to isolate relatively fast-growing bacteria. After the visual enumeration of bacterial isolates, single colonies were picked and streaked onto MPA and this process was repeated until the pure cultures of bacteria were obtained.

2.4.2 | Long-term storage of the fast-growing green snow bacterial isolates

A cryopreservation procedure was used for the long-term storage of bacterial isolates obtained from the green snow samples. Bacteria were cultivated on meat peptone broth (MPB), and 100 µl of cell mass was mixed with glycerol (20% of the final volume) in cryovials and stored at −80°C.

2.4.3 | Microscopy evaluation and identifying optimal growth temperature

For the microscopy evaluation, bacteria were grown on brain–heart infusion (BHI) agar for 3–5 days at 18°C. The cell morphology of green

snow fast-growing bacteria was studied by examining Gram-stained cells using widefield microscope Leica DM4 B (Leica Microsystems, Germany) with an objective magnification of ×100 (Harisha, 2007). For identifying the optimal growth temperature, bacteria were cultivated on MPA at temperatures 4°C, 10°C, 18°C, 25°C, and 37°C for 10 days with the daily evaluations of the growth by microscopy with widefield microscope Leica DM4 B (Leica Microsystems, Germany) and objective magnification of ×100 (Harisha, 2007), the colonies larger than 1.0 mm were visually evaluated. The evaluation of growth was performed according to the score-based scale where score “0” indicates the absence of growth, score “1–2” indicates a little growth, score “3–4” indicates relatively good growth without single colonies, score “5–6” indicates the growth with the single colonies 0.5–1.0 mm in diameter, score “7–8” indicates the growth when the diameter of colonies was 1.5–2.0 mm, and score “9–10” indicates the growth when the diameter of colonies was higher than 2.5 mm.

2.4.4 | Screening for the enzymatic activity

Enzymatic activity was evaluated by applying plate-based assays where bacteria were incubated on selective agar media for 48 h at 18°C, and the diameter of enzyme-specific zones surrounding bacterial colonies was measured. The incubation time of 48 h was chosen because after prescreening, it was observed that the enzymatic activity possessed by the isolated bacteria was detectable after 48 h, while bacteria not showing any enzymatic activity did not show it even after 7 days of incubation. The lipase activity was determined using incubation on MPA containing 1% (v/v) Tween-80 or Tween-20 with the subsequent measurement of the precipitation zones. The amylolytic activity was determined by the incubation on MPA with 0.2% soluble starch, and clearing zones were measured after flooding with iodine (Lugol's solution). The cellulolytic activity was determined using incubation on MPA containing 0.1% sodium carboxymethyl cellulose, and the formation of bright or transparent zones was measured after pouring 0.1% Congo red and subsequent washing with 8% NaCl solution. The proteolytic activity was determined using incubation on calcium–casein agar (Conda, Spain) and subsequently measuring the diameter of clear zones. DNase activity was determined using DNase test agar (Conda, Spain) and evaluating the size of colorful zones.

2.4.5 | Sample preparation for 16S rRNA gene sequencing

To identify fast-growing green snow bacterial isolates, the near-full-length 16S rRNA gene was amplified and sequenced. For the 16S rRNA gene sequencing, isolated bacteria were cultivated on MPA at 18°C for 3–5 days depending on the isolate. A bacterial DNA Preparation Kit (Jena Biosciences, Germany) was used for extracting genomic DNA, according to the instructions of the

manufacturer. The amplification of the 16S rRNA gene was performed by the polymerase chain reaction (PCR) using the universal eubacterial primers 8f (5'-agagtttgatcctggctcag-3') and 1492r (5'-gggttacctgttaccgactt-3') (Lane, 1991), provided by Primetech (Minsk, Belarus). Each 50 µl reaction volume contained 20 µl of 2.5× HF reaction buffer (Institute of Microbiology of National Academy of Science of Belarus), 1 µl of each primer with the concentration 10.0 pmol, 1 µl of bacterial DNA, 26.5 µl of H₂O (MiliQ), and 0.5 µl of proofreading DNA polymerases Diamond (2 U/µl) (Institute of Microbiology of National Academy of Science of Belarus), which was used for high accuracy of amplification. Amplification conditions were as follows: 98°C for 5 min (1 cycle); 98°C for 20 s, 57°C for 20 s, and 72°C for 90 s (30 cycles); 72°C for 3 min (1 cycle); and cooling to 4°C. Purified PCR products were Sanger-sequenced in separate reactions using several internal primers, provided by Primetech (Minsk, Belarus): 926R-seq (5'-ccgtcaattcatttgagttt-3'), 336F-seq (5'-acggyccagactcctacg-3'), 522R-seq (5'-tattaccgcg-gctgctggcac-3'), and 918F-seq (5'-actcaaakgaattgacggg-3') (Lane, 1991). DNA Cycle Sequencing Kit (Jena Bioscience, Germany) was applied for the sequencing reactions, and DNA Analyzer Li-COR 4300 (Li-COR Biosciences, USA) was used for electrophoresis and analysis of the sequencing products.

2.4.6 | Analysis of 16S rRNA gene sequencing data

The processing of 16S rRNA gene sequencing data, editing them, and rendering it on FASTA format was performed using the e-Seq™ Software V. 3.1.10 (Li-COR Biosciences, USA). All sequences of each isolate were aligned using AlignIR 2.1 (Li-COR Biosciences, USA) to obtain a consensus sequence. Comparative analysis of nucleotide sequences of 16S rRNA genes of isolated bacteria and reference sequences was performed using the EzBioCloud database (Yoon et al., 2017). The phylogenetic tree was built using the MEGA7 software (Kumar et al., 2018) with bootstrap values generated from 1000 replicates using the maximum-likelihood method and Tamura-Nei model (Tamura & Nei, 1993). Bootstrap values greater than 70% were shown. The type strain *Methanosarcina barkeri* Schnellen 1947 was chosen as a root for the phylogenetic tree. The closest neighbors and type strain from the EzBioCloud database were included in the tree.

2.4.7 | Identifying the presence of DNA replicons

The presence of DNA replicons was evaluated using 0.7% agarose gel in the TAE buffer stained with ethidium bromide. *Escherichia coli* XL1-Blue [pUC18] (Collection of Microorganisms, Faculty of Biology, Belarusian State University) was used as a control for the determination of DNA plasmids in the bacterial genome. Molecular weight marker GeneRuler DNA Ladder Mix (Thermo Fisher, SM0331) was used for the determination of replicons' size. Further, gels were examined using the ChemiDoc MP Imaging System (Bio-Rad

Laboratories, USA). The detection of DNA replicons was done using densitometry analysis of images by using ImageLab software version 6.0 (Bio-Rad Laboratories, USA).

2.4.8 | Cultivation of fast-growing bacteria for biochemical phenotyping by FTIR spectroscopy

The cultivation of bacteria for FTIR spectroscopic biochemical phenotyping was performed on BHI agar and BHI broth (Sigma-Aldrich, India) media. Cultivation on BHI agar was performed at 18°C for 3–5 days depending on the isolate. Cultivation in BHI broth was performed for 7 days for all isolates at 18°C with 250 rpm agitation speed in the Duetz Microtiter Plate System—Duetz-MTPS (Enzymscreen, the Netherlands), consisting of 24-square polypropylene deep well plates, low-evaporation sandwich covers, and extra high cover clamps (Byrtusová et al., 2020; Duetz et al., 2000; Dzurendova, et al., 2020a; Dzurendova, et al., 2020b; Kosa, Kohler, et al., 2017; Kosa, Vuoristo, et al., 2018). Duetz-MTPS was mounted on the shaking platform of an Innova 40R refrigerated desktop shaker (Eppendorf, Germany). All cultivation for FTIR analysis was done in three biological replicates. Independent agar and broth cultivation were performed on different days.

After the cultivation, bacterial biomass was collected and washed with distilled water three times by applying centrifugation with 25.200 g at 4°C for 5 min. Further, at the last washing step, 50–100 µl of distilled water was added to the cell pellet and resuspended. 8–10 µl of the obtained cell suspension was transferred onto IR-light-transparent silicon 384-well microplates (Bruker Optik, Germany) in three technical replicates. Samples were dried at room temperature for 45–60 min. FTIR spectroscopy analysis was performed using a High-throughput Screening eXTension (HTS-XT) unit coupled to a Vertex 70 FTIR spectrometer (both Bruker Optik, Germany) allowing to perform high-throughput screening (HTS) transmission mode measurements. The spectra were recorded in the region between 4000 and 500 cm⁻¹ with a spectral resolution of 6 cm⁻¹ and an aperture of 5.0 mm.

2.4.9 | Analysis of FTIR spectral data

Before multivariate analysis, the FTIR data were preprocessed. The preprocessing of FTIR data was done in the following way: (1) preprocessing of the entire spectral region by using the second derivative calculated using the Savitzky–Golay algorithm (Savitzky & Golay, 1964) with window size 11, second polynomial order, and 9 smoothing points, followed by (2) splitting of the data into three informative regions: 3050–2800 cm⁻¹ and 1800–1700 cm⁻¹, 1700–1500 cm⁻¹, and 1200–700 cm⁻¹, followed by (3) preprocessing by Extended Multiplicative Signal Correction (EMSC) for every spectral region separately (Kohler et al., 2005, 2020; Liland et al., 2014; Tafintseva et al., 2020; Zimmermann & Kohler, 2013). Different spectral regions

were preprocessed separately by EMSC to standardize one spectral region at the time. This allows us to standardize for the total lipid content when considering the region 3050–2800 cm^{-1} and 1800–1700 cm^{-1} and thereby highlighting the lipid profile differences in subsequent multivariate analysis. Further, principal component analysis (PCA) and consensus multiblock PCA were applied to the preprocessed spectral data (Hanafi et al., 2011; Hassani et al., 2013). For inspecting spectral bands in FTIR spectra, we performed EMSC on the raw spectra for the standardization (Kohler et al., 2005).

3 | RESULTS AND DISCUSSION

3.1 | Bacterial biomass in green snow

By applying epifluorescence microscopy, we determined the number and total biomass of bacteria in green snow samples. It was observed that green snow sample 2 (G.S.S2) contained a significantly higher number of bacteria (2.71 ± 0.64 million cells/ml), and subsequently, it showed higher bacterial biomass (0.730 ± 0.301 mg/ml) than green snow sample 1 (G.S.S1) (Table 1). This might be related to a location of a penguin colony near the sampling site for G.S.S 2, where the penguin dropping could contribute to the increase in the bacterial biomass in this sample. The effect of penguin dropping on the increasing amount of bacterial population in the Antarctic lake sediment core was reported previously (Li et al., 2006).

3.2 | Bacteria inhabiting green snow according to the amplicon sequences of 16S rRNA genes

An amplicon sequence 16S rRNA gene analysis of bacterial communities of two Antarctic green snow samples showed that most bacteria inhabiting G.S.S1 were bacteria from the phylum *Proteobacteria* (51.09%) represented by the families *Burkholderiaceae* (32.85%) and *Pseudomonadaceae* (17.66%), phylum *Bacteroidetes* (31.49%) represented by the family *Flavobacteriaceae* (22.98%), and phylum *Firmicutes* (12.50%) represented by the family *Clostridiaceae* (10.00%), while G.S.S2 was characterized by a higher content of bacteria from phylum *Proteobacteria* (70.70%) represented by the families *Burkholderiaceae* (46.31%), *Pseudomonadaceae* (13.93%), and *Enterobacteriaceae* (6.94%) and lower content of bacteria from phylum *Bacteroidetes* (25.16%) represented by the families *Weeksellaceae* (10.65%), *Sphingobacteriaceae* (7.35%), and *Flavobacteriaceae* (6.92%) and phylum *Firmicutes* (2.99%) represented by the family

Lachnospiraceae (2.59%) (Tables S1 and S2 <https://doi.org/10.5281/zenodo.4297982>). Bacteria of other phyla were represented at a lower percentage in both samples. A detailed list of all bacteria detected using sequence analysis is presented in supplemental tables (<https://doi.org/10.5281/zenodo.4297982>) and Figures A1 and A2.

Similar results were reported by Terashima et al., where, based on the 16S rRNA gene sequencing of green snow samples from two locations near Lake Sugatami on Mount Asahi in the Daisetsu National Park (Hokkaido, Japan), *Proteobacteria* accounted for approximately 80% of all bacterial communities represented by subphylum *Betaproteobacteria* and order *Burkholderiales* with genera *Actinimicrobium*, *Herminiimonas*, *Glaciimonas*, *Aquaspirillum* and *Polaromonas*, and *Firmicutes* represented by the *Sphingobacteriaceae* family dominated over *Bacteroidetes* (Terashima et al., 2017). Because green snow samples were taken from different places and environments, it is obvious that we observe different results than Terashima et al., but it can be noted that bacteria from phylum *Proteobacteria* could be considered common colonizers of colored snow as they are reported in different studies.

3.3 | Phylogenetic relationships of isolated green snow bacteria by 16S rRNA gene sequencing

The analysis of 16S rRNA gene sequences of 45 bacteria isolated from green snow showed a high similarity with the sequences of isolated and identified bacteria from the EzBioCloud database with the percentage of similarity higher than 98.70% (Figure 2, Table 2). Culturable bacteria isolated from green snow samples belonged to two phyla—*Actinobacteria* (77.8%) and *Proteobacteria* (22.2%)—and represented by six families—*Microbacteriaceae* (46.7%), *Micrococcaeae* (22.2%), *Pseudomonadaceae* (13.3%), *Nocardiaceae* (8.9%), *Moraxellaceae* (6.7%), and *Commamonadaceae* (2.2%). The major identified genera are represented in Table 2. Isolates of *Leifsonia* genus were identified as *L. antarctica*, *L. rubra*, and *L. kafiensis*—psychrophilic bacteria, originally discovered in sediment and pond in Antarctica, and Kafni glacier of the Himalayas (Pindi et al., 2009; Reddy et al., 2003). Genus *Cryobacterium* was represented by species *C. soli* and *C. arcticum* described as psychrotolerant soil bacteria (Bajerski et al., 2011; Gong et al., 2020). The species affiliation for most of the isolates from genera *Arthrobacter*, *Pseudomonas*, *Rhodococcus*, *Salinibacterium*, and *Polaromonas* was not determined due to the low discriminative ability of 16S rRNA gene sequence analysis.

While the phylogenetic composition of bacterial communities of snow varies depending on the physical and chemical factors of environmental conditions, air mass trajectory, and geographical regions (Chuvochina et al., 2009; Fierer et al., 2008; Möhler et al., 2007), our results obtained from 16S rRNA gene sequencing of 45 fast-growing bacteria isolated from green snow are to some extent in accordance with the previously reported findings. For example, many bacterial isolates obtained from the Tibetan Plateau (Liu et al., 2009), green snow of the Daisetsu National Park (Hokkaido, Japan) (Terashima et al., 2017),

TABLE 1 Number of bacteria and bacterial biomass in green snow samples

Green snow samples	Number of bacteria, million cells/ml	Bacterial biomass, mg/ml
G.S.S1	1.15 ± 0.28	0.381 ± 0.098
G.S.S2	2.71 ± 0.64	0.730 ± 0.301

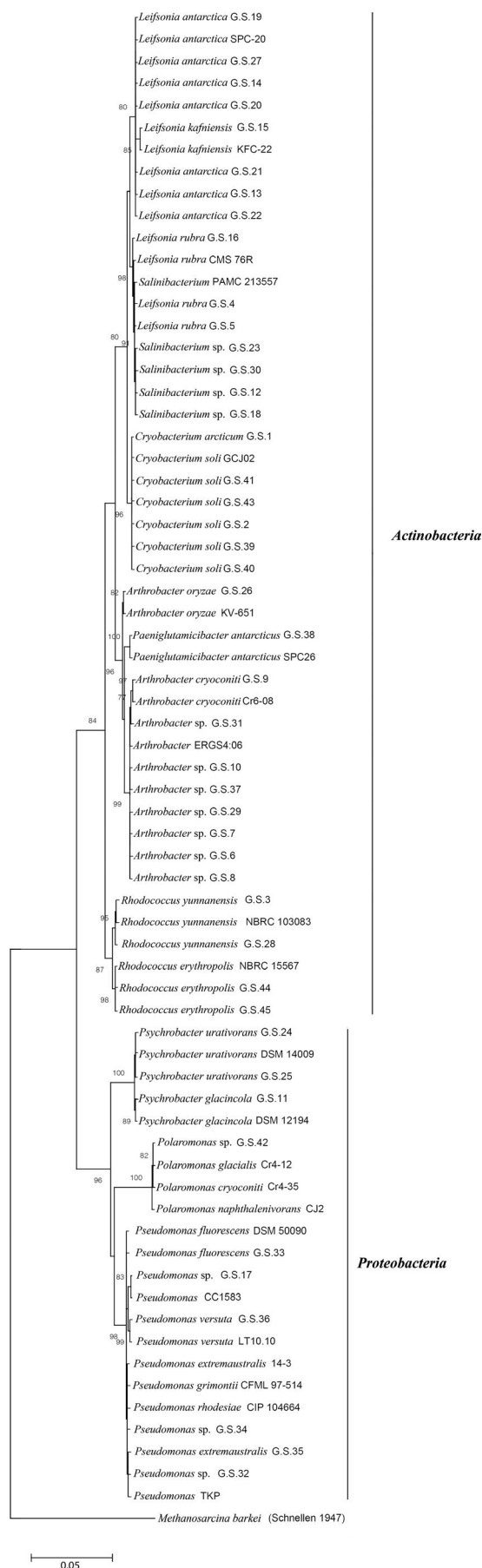


FIGURE 2 Phylogenetic analysis by the maximum-likelihood method with the number of bootstraps from 1000 replicates, and bootstrap values greater than 70% showing the phylogenetic relationship of the bacteria isolated from green snow of the Eastern part of Antarctica and their closest neighbors and type strain from EzBioCloud database. Type strain *Methanosarcina barkeri* Schnellen 1947 was chosen as a root for the phylogenetic tree

and Swiss Alps snow (Meola et al., 2015) belonged to *Proteobacteria* represented by genus *Polaromonas* similar to our study. Further, it was reported that bacteria from the green snow samples from Ryder Bay, Antarctic Peninsula (Rothera Point, Anchorage Island, Leonie Island, and Lagoon Island), are represented by *Flavobacterium*, *Pedobacter*, *Hymenobacter* *Massilia*, *Polaromonas*, and *Chryseobacterium* genera (Davey et al., 2019). It could be seen that *Polaromonas* bacteria are the common colonizers of green snow from different environments.

Interestingly, 16S rRNA gene sequencing of isolated bacteria and amplicon sequencing analysis of green snow samples revealed different results for the type of predominant bacterial genera present in the analyzed Antarctic green snow samples. This could be because different sequencing techniques for bacteria sequencing and to determine bacteria in snow samples were used. The amplicon 16S rRNA gene sequencing analysis can reveal both fast- and slow-growing bacteria. Thus, according to this analysis, it was shown that genus *Leifsonia* (phylum *Microbacteriaceae*) is the most predominant among the isolated bacteria, while the amplicon 16S rRNA gene sequencing analysis detected only 0.2% of bacteria belonging to phylum *Microbacteriaceae* in G.S.S1 and 0.7% in G.S.S2 (Table S1 and S2 <https://doi.org/10.5281/zenodo.4297982>, Figures A1 and A2). While bacteria from genera *Acidovorax*, *Janthinobacterium*, and *Chryseobacterium* were detected by metagenomic analysis as the most predominant one, the bacteria of these genera were not present among the isolated bacteria. This could be explained by the growth conditions chosen for isolating fast-growing bacteria that were not suitable for bacteria of these genera. The 16S rRNA gene sequencing showed that the second and third predominant genera are *Arthrobacter* and *Cryobacterium*, while the 16S rRNA gene amplicon sequencing analysis showed that these genera were present at a low quantity of approximately 1.05% and 0.64%, respectively. This could be an indication that bacteria of these genera have a high ability to grow in a culture. The presence of *Pseudomonas* bacteria was in agreement between both methods.

3.4 | The presence of DNA replicons

All bacterial isolates were screened for the presence of DNA replicons, where *Escherichia coli* XL1-Blue with the plasmid pUC18 was used as a reference strain to determine extrachromosomal DNA. It was observed that eight green snow bacterial isolates contain several DNA replicons (plasmids or chromosomes): (1) Isolates *Cryobacterium arcticum* G.S.1, *Cryobacterium soli* G.S.2, G.S.39, and G.S.40 and isolates *Arthrobacter* sp. G.S.7, G.S.29, and G.S.37 had a large DNA replicon with a size of more than 10 kilobase pairs (kbp); and (2) isolate *Psychrobacter glacinicola* G.S.11 contained several

TABLE 2 Phylogenetic relationships, optimal growth temperature, and enzymatic activity of the bacteria isolated from the Antarctic green snow samples

Phylum	Snow sample/Isolate GenBank Accession number	Closest EzBioCloud relative	Similarity %	Enzymatic activity 1 2 3 4 5 6					
Actinobacteria	G.S.S2/ G.S.1 ^{a,c,d,e} /MT890158	<i>Cryobacterium arcticum</i> SK-1	99.78						
	G.S.S2/ G.S.2 ^{a,c,d,e} /MT890159	<i>Cryobacterium soli</i> GCJ02	99.86						
	G.S.S2/ G.S.3 ^{a,c,d,e} /MT890160	<i>Rhodococcus yunnanensis</i> NBRC 103083	99.38						
	G.S.S2/ G.S.4 ^{a,c,d,e} /MT890161	<i>Leifsonia rubra</i> CMS 76R	99.10						
	G.S.S2/ G.S.5 ^{a,c,d,e,f} /MT890162	<i>Leifsonia rubra</i> CMS 76R	99.25						
	G.S.S2/ G.S.6 ^{a,c,d,e} /MT890163	<i>Arthrobacter</i> ERGS4:06	99.51						
		<i>Arthrobacter</i> <i>psychrochitiniphilus</i> GP3	99.32 99.23						
		<i>Arthrobacter glacialis</i> HLT2-12-2							
	G.S.S2/ G.S.7 ^{a,c,d,e,f} /MT890164	<i>Arthrobacter</i> ERGS4:06	99.51						
		<i>Arthrobacter</i> <i>psychrochitiniphilus</i> GP3	99.32 99.23						
		<i>Arthrobacter glacialis</i> HLT2-12-2							
	G.S.S2/ G.S.8 ^{a,c,d,e} /MT890165	<i>Arthrobacter</i> ERGS4:06	99.51						
		<i>Arthrobacter</i> <i>psychrochitiniphilus</i> GP3	99.32 99.23						
		<i>Arthrobacter glacialis</i> HLT2-12-2							
	G.S.S1/ G.S.9 ^{a,c,d,e} /MT890166	<i>Arthrobacter cryoconiti</i> Cr6-08	98.97						
	G.S.S1/ G.S.10 ^{a,c,d,e} /MT890167	<i>Arthrobacter</i> ERGS4:06	99.52						
		<i>Arthrobacter</i> <i>psychrochitiniphilus</i> GP3	99.34 99.25						
		<i>Arthrobacter glacialis</i> HLT2-12-2							
	G.S.S1/ G.S.12 ^{a,c,d,e,f} /MT890169	<i>Salinibacterium</i> PAMC 21357	99.38						
		<i>Salinibacterium</i> UTAS2018	99.03						
	G.S.S1/ G.S.13 ^{a,c,d,e} /MT890170	<i>Leifsonia antarctica</i> SPC-20	100						
	G.S.S1/ G.S.14 ^{a,c,d,e} /MT890171	<i>Leifsonia antarctica</i> SPC-20	100						
	G.S.S1/ G.S.15 ^{a,c,d,e,f} /MT890172	<i>Leifsonia kafniensis</i> KFC-22	99.65						
	G.S.S1/ G.S.16 ^{a,c,d,e} /MT890173	<i>Leifsonia rubra</i> CMS 76R	99.45						
	G.S.S1/ G.S.18 ^{a,c,d,e,f} /MT890175	<i>Salinibacterium</i> PAMC 21357	99.38						
		<i>Salinibacterium</i> UTAS2018	99.17						
	G.S.S1/ G.S.19 ^{a,c,d,e,f} /MT890176	<i>Leifsonia antarctica</i> SPC-20	100						
	G.S.S1/ G.S.20 ^{a,c,d,e,f} /MT890177	<i>Leifsonia antarctica</i> SPC-20	100						
	G.S.S1/ G.S.21 ^{a,c,d,e,f} /MT890178	<i>Leifsonia antarctica</i> SPC-20	99.58						

(Continues)

TABLE 2 (Continued)

Phylum	Snow sample/Isolate GenBank Accession number	Closest EzBioCloud relative	Similarity %	Enzymatic activity 1 2 3 4 5 6					
Proteobacteria	G.S.S1/ G.S.22 ^{a,c,d,e,f} /MT890179	<i>Leifsonia antarctica</i> SPC-20	99.93						
	G.S.S1/ G.S.23 ^{a,c,d,e,f} /MT890180	<i>Salinibacterium</i> PAMC 21357 <i>Salinibacterium</i> UTAS2018	99.44 99.24						
	G.S.S1/ G.S.26 ^{b,c,d,e,f} /MT890183	<i>Arthrobacter oryzae</i> KV-651	99.03						
	G.S.S1/ G.S.27 ^{a,c,d,e,f} /MT890184	<i>Leifsonia antarctica</i> SPC-20	100						
	G.S.S1/ G.S.28 ^{b,c,d,e,f} /MT890185	<i>Rhodococcus yunnanensis</i> NBRC 103083	99.10						
	G.S.S1/ G.S.29 ^{a,c,d,e,f} /MT890186	<i>Arthrobacter</i> ERGS4:06 <i>Arthrobacter</i> <i>psychrochitiniphilus</i> GP3 <i>Arthrobacter glacialis</i> HLT2-12-2	99.52 99.34 99.31						
	G.S.S1/ G.S.30 ^{a,c,d,e,f} /MT890187	<i>Salinibacterium</i> PAMC 21357 <i>Salinibacterium</i> UTAS2018	99.24 99.03						
	G.S.S1/ G.S.31 ^{a,c,d,e} /MT890188	<i>Arthrobacter</i> ERGS4:06	98.76						
	G.S.S2/ G.S.37 ^{a,c,d,e,f} /MT890194	<i>Arthrobacter</i> ERGS4:06 <i>Arthrobacter</i> <i>psychrochitiniphilus</i> GP3 <i>Arthrobacter glacialis</i> HLT2-12-2	99.51 99.23 99.23						
	G.S.S2/ G.S.38 ^{a,c,d,e} /MT890195	<i>Paeniglutamicibacter</i> <i>antarcticus</i> SPC26	100						
	G.S.S1/ G.S.39 ^{a,c,d,e,f} /MT890196	<i>Cryobacterium soli</i> GCJ02	99.93						
	G.S.S1/ G.S.40 ^{a,c,d,e,f} /MT890197	<i>Cryobacterium soli</i> GCJ02	99.93						
	G.S.S2/ G.S.41 ^{a,c,d,e,f} /MT890198	<i>Cryobacterium soli</i> GCJ02	99.65						
	G.S.S2/ G.S.43 ^{a,c,d,e,f} /MT890200	<i>Cryobacterium soli</i> GCJ02	99.72						
	G.S.S2/ G.S.44 ^{a,c,d,e,f} /MT890201	<i>Rhodococcus erythropolis</i> NBRC 15567	100						
	G.S.S2/ G.S.45 ^{a,c,d,e,f} /MT890202	<i>Rhodococcus erythropolis</i> NBRC 15567	100						
	G.S.S1/ G.S.11 ^{b,c,d,e} /MT890168	<i>Psychrobacter glacinicola</i> DSM 12194	99.18						
	G.S.S1/ G.S.17 ^{b,c,d,e,f} /MT890174	<i>Pseudomonas</i> CC1583 <i>Pseudomonas cannabina</i> CFBP 2341 <i>Pseudomonas mandelii</i> MBRC 103147	99.11 99.04 99.04						
	G.S.S1/ G.S.24 ^{b,c,d,e} /MT890181	<i>Psychrobacter urativorans</i> DSM 14009	99.93						
	G.S.S1/ G.S.25 ^{b,c,d,e} /MT890182	<i>Psychrobacter urativorans</i> DSM 14009	99.93						

(Continues)

TABLE 2 (Continued)

Phylum	Snow sample/Isolate GenBank Accession number	Closest EzBioCloud relative	Similarity %	Enzymatic activity 1 2 3 4 5 6					
				1	2	3	4	5	6
	G.S.S1/	<i>Pseudomonas</i> TKP	99.59						
	G.S.32 ^{b,c,d,e,f} /MT890189	<i>Pseudomonas veronii</i> DSM 11331	99.52						
		<i>Pseudomonas extremaustralis</i> 14-3	99.52						
	G.S.S2/	<i>Pseudomonas fluorescens</i> DSM 50090	99.93						
	G.S.33 ^{b,c,d,e,f} /MT890190								
	G.S.S2/	<i>Pseudomonas grimontii</i> CFML 97-514	99.93						
	G.S.34 ^{b,c,d,e,f} /MT890191	<i>Pseudomonas rhodesiae</i> CIP 104664	99.79						
		<i>Pseudomonas extremaustralis</i> 14-3	99.73						
		<i>Pseudomonas marginalis</i> ATCC 10844	99.63						
	G.S.S2/	<i>Pseudomonas extremaustralis</i> 14-3	99.66						
	G.S.35 ^{b,c,d,e,f} /MT890192								
	G.S.S2/	<i>Pseudomonas versuta</i> LT10.10	100						
	G.S.36 ^{b,c,d,e,f} /MT890193								
	G.S.S2/	<i>Polaromonas glacialis</i> Cr4-12	99.24						
	G.S.42 ^{b,c,d,e} /MT890199	<i>Polaromonas cryconite</i> Cr4-35	99.24						
		<i>Polaromonas naphthalenivorans</i> CJ2	99.10						

Note: 1—Protease activity, 2—amylolytic activity, 3—cellulolytic activity, 4—DNase activity, 5—lipolytic activity (Tween-20), 6—lipolytic activity (Tween-80). Gray color—the presence of enzymatic activity, black color—the absence of enzymatic activity.

^aGram-positive.

^bGram-negative.

^c4°C.

^d10°C.

^e18°C.

^f28°C.

^g37°C.

high molecular replicons (more than 10 kbp) and one or two plasmids with a size lower than 10 kbp (Figure A3).

The presence of DNA replicons for these species was reported previously (Bajerski et al., 2011; Kageyama et al., 2008; Pindi et al., 2010; Shivaji et al., 2004). Thus, it was shown that the genomes of *Cryobacterium arcticum* strain PAMC 27867 and *Psychrobacter* spp. strains, isolated from Arctic soil (sedimentary rock) have two circular plasmids in size from 117.792 bp to 58.936 bp (Lee et al., 2016) and from 2.9 to 14.9 kbp (Dziewit et al., 2013), respectively. The presence of DNA replicons in Antarctic green snow bacteria could be explained by their need for adaptation to extreme environmental conditions (Romaniuk et al., 2018).

3.5 | Cell morphology and optimal growth temperature

Cell morphology of Antarctic green snow bacteria was studied by widefield microscopy evaluation of Gram-stained cells, and we

present microscopy images for nine typical isolates representing all genera (Figure A4). The observed cell morphology was in accordance with the previously reported cell morphology (Bajerski et al., 2011; Busse, 2016; Gordon et al., 1974; Kageyama et al., 2008; Margesin et al., 2012; Pindi et al., 2009, 2010; Shivaji et al., 2004; Wang et al., 2009; Zhang et al., 2005).

The isolated green snow bacteria showed good growth at a wide temperature range between 4°C and 28°C, and while they did not grow at 37°C (Table 2), this characterizes them as facultative psychrophiles. Generally, growth temperature optima for nearly all isolates were in accordance with the previously reported values for the respective type strains (Gordon et al., 1974; Reddy et al., 2003; Shivaji et al., 2004; Zhang et al., 2005). All bacteria isolated from green snow showed good growth at 4°C and 10°C (Table 2). Further, all isolates except *Polaromonas* sp. G.S.42 could grow at 18°C. The isolates *Arthrobacter* sp. G.S.6, G.S.7, G.S.8, and G.S.37, *Pseudomonas* sp. G.S.32, *Pseudomonas fluorescens* G.S.33, *Pseudomonas* sp. G.S.34, *Pseudomonas extremaustralis* G.S.35, *Pseudomonas versuta* G.S.36, and *Paeniglutamicibacter antarcticus* G.S.38 showed equally good

growth at 4°C and 10°C (Table 2). High growth ability at 28°C was obtained only for the isolates *Pseudomonas* sp. G.S.17, G.S.32, and G.S.34 *Pseudomonas fluorescens* G.S.33, *Pseudomonas extremaustralis* G.S.35, *Pseudomonas versuta* G.S.36, *Arthrobacter oryzae* G.S.26, *Leifsonia antarctica* G.S.27, *Rhodococcus yunnanensis* G.S.28, and *Rhodococcus erythropolis* G.S.44 and G.S.45, while other isolates could not grow or were characterized by the slow growth at this temperature (Table 2). For most of the isolates identified at the genus level only, our results are well correlating with the previously reported (Bajerski et al., 2011; Wang et al., 2009; Zhang et al., 2005).

3.6 | Enzymatic activity

Screening for the enzymatic activity of isolated green snow bacteria was performed by the plate-based assays for the following enzymes: protease, amylase, cellulase, DNase, and lipase, and results are presented in Table 2. All Antarctic green snow bacteria were characterized by the enzymatic activity of at least one enzyme, excluding isolates *Arthrobacter* sp. G.S.6, *Paeniglutamicibacter antarcticus* G.S.38, and all isolates of genus *Salinibacterium* and *Leifsonia*, except *Leifsonia rubra* G.S.5 and *Leifsonia kafniensis* G.S.15 (Table 2). In particular, a does high level of enzymatic activity, with more than two enzymes produced, was observed for all isolates of genera *Cryobacterium* and *Pseudomonas* and some isolates of genera *Arthrobacter* (Table 2). More than half of enzymatically active green snow bacteria showed lipolytic activity, where all *Psychrobacter* and *Rhodococcus* isolates, except *Rhodococcus yunnanensis* G.S.3, most isolates of genera *Arthrobacter* and *Pseudomonas*, and isolates *Leifsonia kafniensis* G.S.15, and *Polaromonas* sp. G.S.42 could hydrolyze both Tween-20 and Tween-80 (Table 2). Interestingly, all isolates of genus *Cryobacterium* could hydrolyze only Tween-20 (Table 2).

DNase activity was detected for all isolates of genus *Pseudomonas* for the isolate *Psychrobacter glacinicola* G.S.11 and some isolates of the genus *Arthrobacter* (Table 2). The amylolytic activity was detected only for bacteria of the genus *Cryobacterium* and the isolate *Arthrobacter* sp. G.S.8 (Table 2). The proteolytic activity was detected for all isolates of genus *Pseudomonas* and isolate *Arthrobacter* sp. G.S.26 (Table 2). The enzymatic activity of isolated Antarctic green snow bacteria identified on the species level was in agreement with previously published results for the strains of the same species isolated from other environments (Kageyama et al., 2008; Pindi et al., 2009; Reddy et al., 2003).

3.7 | Biochemical phenotyping using Fourier transform infrared (FTIR) spectroscopy

3.7.1 | FTIR profile of green snow Antarctic bacteria

The obtained FTIR spectral profiles of the Antarctic green snow bacteria under study cultivated on agar and broth showed clear differences in certain spectral regions. For visualizing the most typical isolate/species related biochemical differences in respective spectral regions, we show two representative FTIR spectra of the isolates *Rhodococcus yunnanensis* G.S.3 and *Arthrobacter* sp. G.S.29 cultivated on agar (Figure 3a, Table 3). FTIR spectra of microbial cells reveal information about cellular lipids, proteins, and polysaccharides (Figure 3a, Table 3). Lipids are described by the spectral regions 3010–2800 cm^{-1} , 1800–1700 cm^{-1} , and some single peaks related to $-\text{CH}_2$ and $-\text{CH}_3$ scissoring in the region 1400–1300 cm^{-1} (Table 3). The most important lipid-associated peaks usually present in FTIR spectra of microorganisms (Guillén et al., 1998; Hong et al., 1999; Naumann, 2000) are as follows: (i) Peaks at 2947 cm^{-1} , 2923 cm^{-1} ,

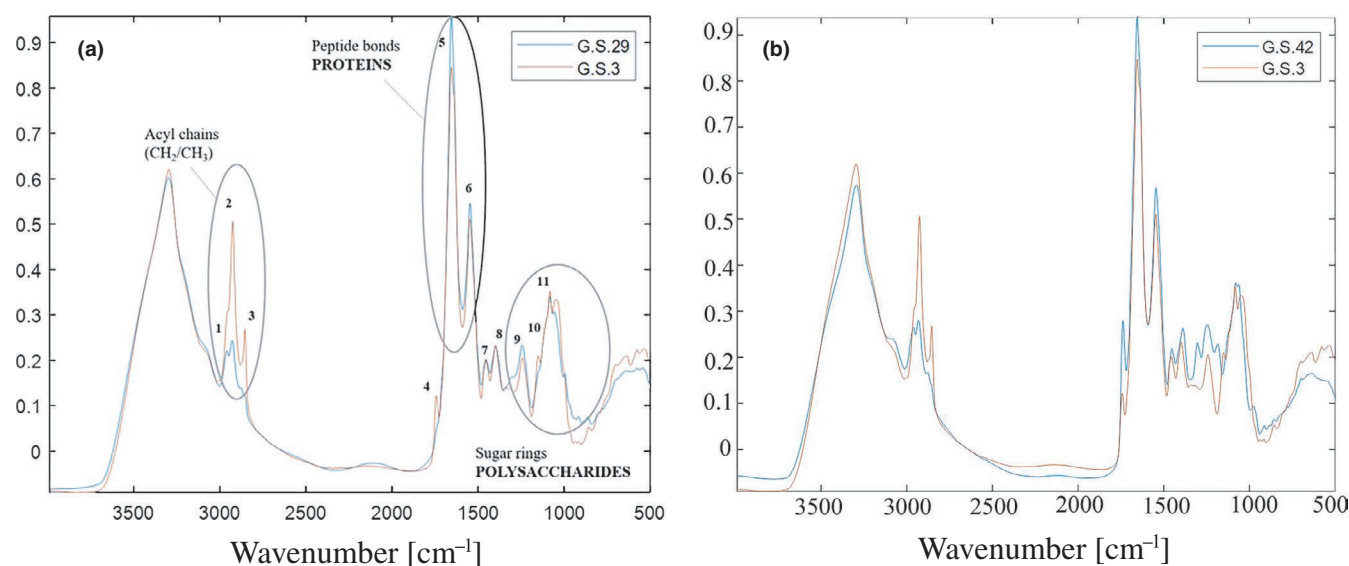


FIGURE 3 EMSC corrected FTIR-HTS spectra of (a) isolate *Rhodococcus yunnanensis* G.S.3 and *Arthrobacter* sp. G.S.29 cultivated on BHI-agar, (b) isolates *Rhodococcus yunnanensis* G.S.3 and *Polaromonas* sp. G.S.42 cultivated on BHI agar. The numbers indicating respective peak assignments described in Table 3

TABLE 3 Peak assignments for the FTIR-HTS spectra of Antarctic green snow bacteria

Peak number ^a	Wavenumber (cm ⁻¹)	Peak assignment	References
1	2947	-C-H (CH ₃) stretching in lipids and hydrocarbons	Guillén et al. (1998)
2	2923	-C-H (CH ₂) stretching	Hong et al. (1999)
3	2847	CH ₂ /CH ₃ stretching in lipids and hydrocarbons	Guillén et al. (1998)
4	1739, 1741, 1747	C = O ester bond stretching in lipids, esters, and polyesters	Hong et al. (1999)
5	1650	-C = O stretching, α -Helix Amide I in proteins	Jackson et al. (1995)
6	1540	N-H bending and C-N stretching, Amide II in proteins	Jackson et al. (1995)
7	1449	CH ₂ /CH ₃ stretching in lipids	Guillén et al. (1998)
8	1394	-C-H (CH ₃) bending (sym) in lipids	Naumann (2000)
9	1239	-P = O stretching of phosphodiester	Naumann (2000)
10	1148	C-O-C/C-O stretching in polysaccharides	Naumann (2000)
11	1075	C-O-C/C-O stretching in polysaccharides	Naumann (2000)

^aPeak number as in Figure 3a.

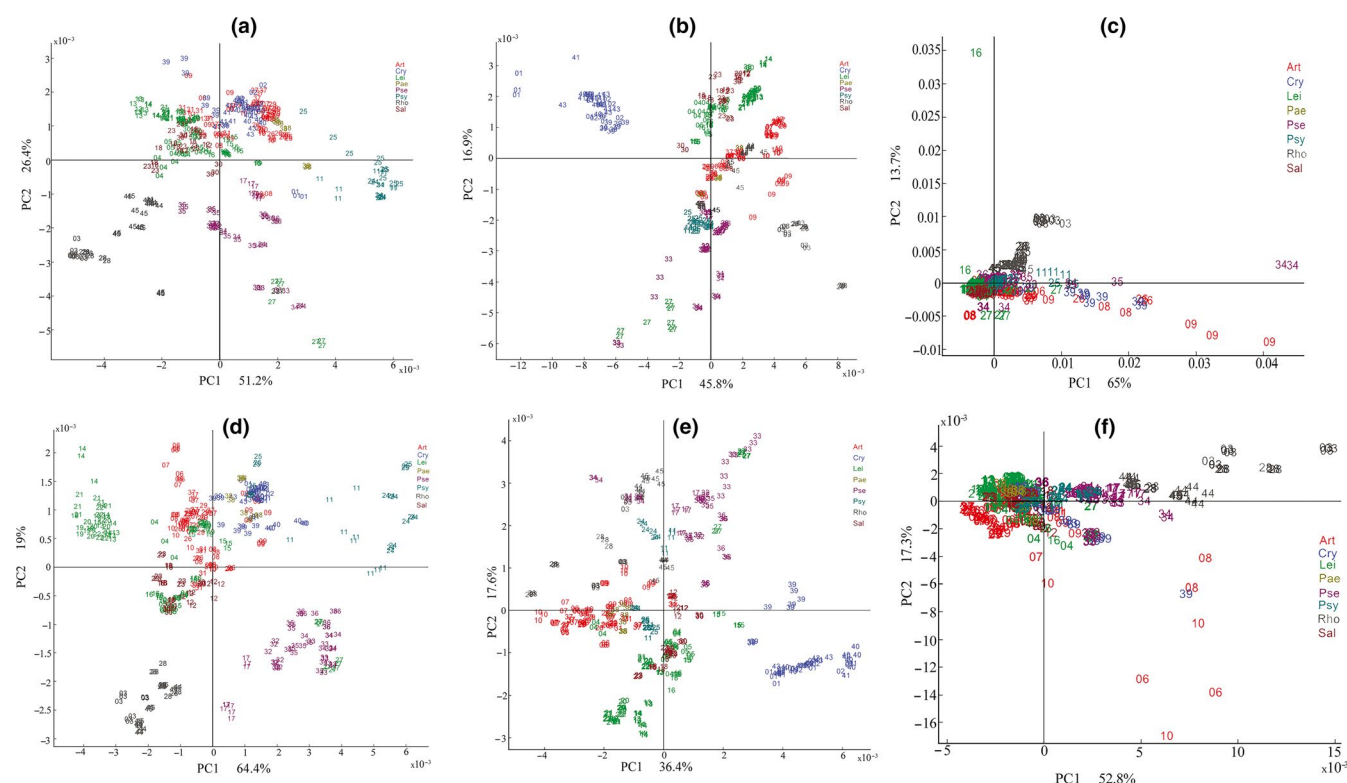


FIGURE 4 PCA scatter plots of lipid/ester/PHA (a and d), polysaccharide (b and e), and protein (c and f) regions of FTIR-HTS spectra of Antarctic green snow bacteria cultivated on BHI agar (a, b, and c) and BHI broth (d, e, and f). The dataset does not contain FTIR-HTS spectra of the isolate *Polaromonas* sp. G.S.42. The numbers on PCA plots indicate samples and are related to the isolate number in G.S. abbreviation (Table 2). The colors of samples on PCA plots are corresponding to the genus abbreviations: Art—*Arthrobacter*; Cry—*Cryobacterium*; Lei—*Leifsonia*; Pae—*Paeniglutamicibacter*; Pse—*Pseudomonas*; Psy—*Psychrobacter*; Rho—*Rhodococcus*; Sal—*Salinibacterium*

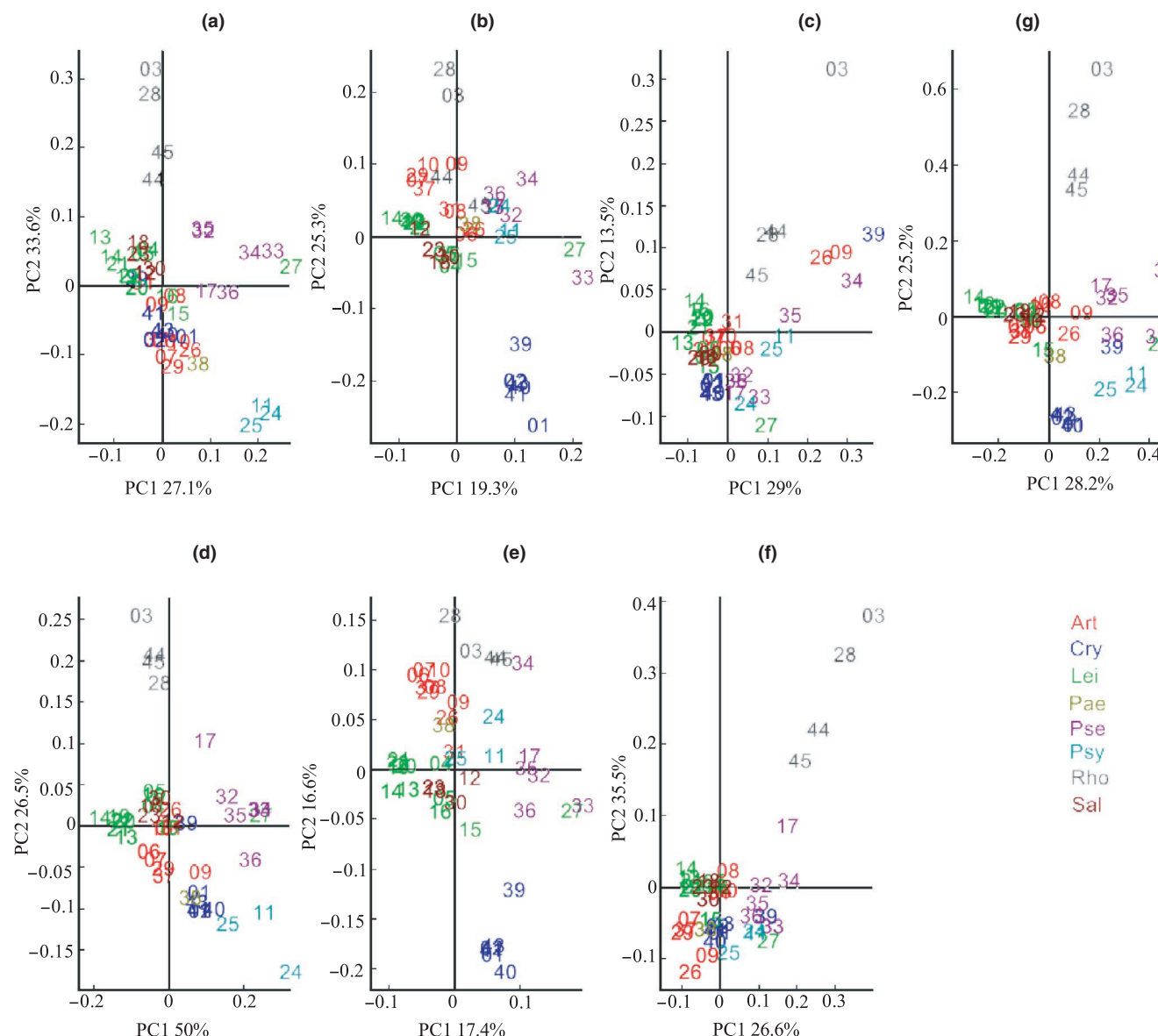


FIGURE 5 Multiblock PCA scatter plots of lipid/ester/PHA (a and d), polysaccharide (b and e), and protein (c and f) regions of FTIR spectra of Antarctic green snow bacteria cultivated on BHI agar (a, b, and c) and BHI broth (d, e, and f). The dataset does not contain FTIR spectra of the isolate *Polaromonas* sp. G.S.42. Multiblock PCA consensus is presented on G. The numbers on PCA plots indicate samples and are related to the isolate number in G.S. abbreviation (Table 2). The colors of samples on PCA plots are corresponding to the genus abbreviations: Art—*Arthrobacter*; Cry—*Cryobacterium*; Lei—*Leifsonia*; Pae—*Paeniglutamicibacter*; Pse—*Pseudomonas*; Psy—*Psychrobacter*; Rho—*Rhodococcus*; Sal—*Salinibacterium*

2847 cm^{-1} , 1449 cm^{-1} , and 1394 cm^{-1} are related to $-\text{CH}_3$ and $-\text{CH}_2$ stretching and mainly indicate the chain length of carbon skeleton in lipid molecules; (ii) the peak at 1745 cm^{-1} is related to the ester bond stretching and indicates the total lipid content in the cell. A shift at this peak to lower wavenumbers is related to the ester bond stretching in esters and can indicate polyhydroxyalkanoates (PHA); (iii) the peak at 1710 cm^{-1} is related to the carboxyl bond vibrations in free fatty acids; (iv) the peak at 3010 cm^{-1} is related to $=\text{C}-\text{H}$ stretching in lipids and indicates the unsaturation level of cellular lipids. In bacterial cells, lipid-associated peaks usually do not exhibit significant absorbance values and some peaks, for example, 3010 cm^{-1} and 1710 cm^{-1} , are not detected. This is because the total lipid content in

bacteria is low because they do not often possess oleaginous properties and the cell membrane is one of the main locations of lipids in the bacterial cells. Notwithstanding, FTIR spectra of some Antarctic green snow bacterial isolates *Rhodococcus yunnanensis* G.S.3 and *Polaromonas* sp. G.S.42 showed absorbance values at $-\text{CH}_3$ and $-\text{CH}_2$ stretching peaks at 2947 cm^{-1} , 2923 cm^{-1} , and 2847 cm^{-1} , and ester bond stretching peak at 1741 cm^{-1} and 1738 cm^{-1} , respectively, indicating esters and possibly polyesters as, for example, polyhydroxyalkanoates (PHA) (Hong et al., 1999) (Figure 3b). The ability to synthesize and accumulate PHA was previously reported for bacterial genera *Rhodococcus* (Altaee et al., 2016) and extremophiles, such as *Polaromonas* (Koller, 2017).

Cellular proteins can be detected in the region 1700–1500 cm^{-1} where peaks related to the amide I (1650 cm^{-1}) and amide II (1540 cm^{-1}) bonds are located (Table 3, Figure 3a). FTIR spectrum of bacterial cells normally exhibits protein peaks as the peaks with the highest absorbance values, which is in accordance with our observations in the FTIR spectra of green snow bacteria, indicating that proteins are the dominant intracellular chemical component of the cells. Further, IR spectra of bacteria reveal the biochemical profile of cellular polysaccharides, which can be observed in the spectral region 1200–900 cm^{-1} and which are related to sugar ring vibrations (Figure 3a, Table 3). The polysaccharide region is often considered a fingerprint region, and is unique for every microbial species/strain and allows us to perform phenotypic identification on different phylogenetic levels (Harz et al., 2009; Naumann, 2000).

3.7.2 | PCA and multiblock analysis of FTIR profiles of green snow bacteria

Isolated green snow bacteria showed clear isolate/species-specific polysaccharide profiles allowing us to separate them into phenotypic groups, as it could be seen in the PCA results (Figure 4b,e, Figures A5B,E). Principal component analysis (PCA) of FTIR spectra obtained for agar- and broth-cultivated green snow bacteria was performed for lipid/ester, protein, and polysaccharide regions separately, and results are shown in Figure 4 and Figure A5. Consensus multiblock PCA was used to perform a combined analysis of agar and broth FTIR spectra (Figure 5 and Figure A6).

PCA scatter plot of all samples shows two groups, where one group is the isolate *Polaromonas* sp. G.S.42, and another group is all other isolates. This indicates that *Polaromonas* isolate has a different biochemical profile than all other isolates (Figure A5). The largest differences were observed for lipid/ester/PHA and polysaccharide regions (Figure A5). This could be because FTIR spectra of this isolate show high absorbance for the shifted ester peak at 1738 cm^{-1} indicating esters or polyesters (polyhydroxyalkanoates (PHA)) (Figure 3B). Interestingly, the lipid/ester/PHA and polysaccharide profile of this isolate grown on BHI broth does not show the same distinct differences (Figure A5D,E). This could be due to the difference in the water activity of agar and broth forms of BHI media, and it is a possible indication, which was observed for the first time in our study, that the synthesis of PHA in *Polaromonas* happens in a response to the change in the water availability/activity of the media (environment). The polysaccharide profile of the broth- and especially agar-cultivated isolates belonging to the genus *Cryobacterium* differs significantly from other isolates (Figure A5B). Protein profiles of the broth- and agar-cultivated isolates showed similar results where isolates belonging to the genus *Rhodococcus* and isolate *Cryobacterium soli* G.S.39 differ from all other isolates (Figure A5C,F). PCA scatter plots of the lipid/ester/PHA, polysaccharide, and protein regions of bacteria cultivated in broth show that some isolates of the genus *Arthrobacter* cluster out of the main cloud indicating their difference in the profile and amount of protein, polysaccharide,

and lipid compounds (Figure A5F). When the protein region was used for the analysis, one spectral replicate for the isolate *Leifsonia rubra* G.S.16 cultivated on BHI agar appeared to be significantly different from other replicates and could be considered an outlier. This can be due to the errors happening during the preprocessing (Kohler et al., 2005; Tafintseva et al., 2020). After this outlier was removed from the dataset, the PCA scatterplot of the protein region did not show any significant change in the sample distribution; therefore, we showed a scatter plot of the protein region without the outlier being removed (Figure 4c and Figure A5C). When FTIR spectra of the isolate *Polaromonas* sp. G.S.42 were removed from the dataset, the PCA scatterplot of the polysaccharide region of FTIR spectra of bacteria cultivated on agar showed a clear separation of nearly all isolates on the genus level (Figure 4b). This revealed phenotypic relationships of the isolated green snow bacteria. Thus, it could be seen that bacteria from genera *Psychrobacter* have similar polysaccharide profile as some species of genera *Pseudomonas*. Likewise, isolate *Rhodococcus erythropolis* G.S.45 is close to *Psychrobacter* and *Pseudomonas* isolates while far from other isolates of the genus *Rhodococcus*. Also, isolates from the genus *Salinibacterium* have a similar polysaccharide profile with bacteria from the genus *Leifsonia*, while the isolate *Leifsonia antarctica* G.S.27 has similarity to the isolates of genus *Pseudomonas* (Figure 4b). Bacteria from genera *Pseudomonas* and *Psychrobacter* are Gram-negative, their cell wall has an outer membrane containing lipopolysaccharide, and they are similar at polysaccharide region (1200–700 cm^{-1}). A similar observation was previously reported in other studies (Naumann, 2000; Novais et al., 2019). While the spectral region between 1200 and 900 cm^{-1} is mainly related to C–O–C and C–O–P stretching vibrations of oligo- and polysaccharides, the region between 900 and 600 cm^{-1} is related to the bands from aromatic ring vibrations of the various nucleotides. This characterizes that region as a “true fingerprint region” (Naumann, 2000), and it contributes to achieving good clustering of isolates on the genus and species level when polysaccharide region (1200–700 cm^{-1}) was used.

The PCA scatterplot of the lipid region for the dataset with the removed spectra of *Polaromonas* sp. G.S.42 shows that bacteria belonging to the genera *Rhodococcus* and *Psychrobacter* have different lipid/ester/PHA profiles than other isolates since they cluster out from the main cloud (Figure 4a). Lipid profiles affect prokaryotic taxonomy (Naumann, 2000; Rainey, 2011). The PCA scatterplot of FTIR spectra derived from bacteria cultivated in broth for the dataset without *Polaromonas* sp. G.S.42 did not show any significantly different results than when the initial dataset was used (Figure 4 and Figure A5).

Multiblock PCA shows that the most informative and discriminative spectral regions for the spectra of bacteria cultivated on broth are lipid/ester/PHA and protein because it has the highest explained variance for PC1 of 46.3% and 31.3%, respectively (Figure A6). The results of the multiblock PCA are similar to the results of the ordinary PCA and show distinct differences in lipid/ester/PHA and polysaccharide profile of agar-cultivated bacteria for the isolate *Polaromonas* sp. G.S.42 (Figure A6A,B), in the

polysaccharide profile of agar- and broth-cultivated bacteria for species of the genus *Cryobacterium* (Figure A6B,E), and protein profile of agar- and broth-cultivated isolates for species of genus *Rhodococcus* (Figure A6C,F).

The multiblock PCA of the spectra from bacteria cultivated on agar, excluding the isolate *Polaromonas* sp. G.S.42, shows low explained variance for PC1 for the polysaccharide region (19.3%) and a higher explained variance for the lipid/ester/PHA (27.1%) and protein (29.0%) regions (Figure 5). The high explained variance for PC1 for lipid/ester/PHA region (50.0%) for isolates cultivated in broth indicating good discrimination of analyzed bacteria on genus and species levels (Figure 5d). The results of the consensus multiblock PCA, when all regions were combined, are shown in Figure 5g and Figure A6G. All isolates from genera *Rhodococcus*, some isolates from genera *Pseudomonas* and *Psychrobacter*, and isolate *Cryobacterium soli* G.S.39 are clustering from other isolates belonging to the same genera indicating the difference between the isolates, both on the genus and on the species level (Figure 5g and Figure A6G). The consensus multiblock PCA scatterplot shows that the difference in the cellular biochemical profile of green snow bacteria is influenced by the regions with high explained variance, meaning lipid/ester/PHA and protein.

4 | CONCLUSIONS

In this study, an extensive characterization of fast-growing bacteria isolated from Antarctic green snow was performed in addition to the amplicon 16S rRNA gene sequencing analysis of two green snow samples. The 16S rRNA gene amplicon sequencing analysis with 16S rRNA gene sequence showed that bacteria of the genus *Pseudomonas* are the most abundant in green snow samples. All bacterial isolates were characterized by a broad range of growth temperatures from 4°C to 25°C, and a significant level of enzymatic activity. The lipolytic activity was found in more than half of the isolates under study. The biochemical profiling by FTIR spectroscopy revealed a possible presence of polyesters (polyhydroxyalkanoates (PHA)) or other lipid compounds in some bacterial isolates. The lipid/ester/PHA and protein spectral regions were the most discriminative for getting the distinct genus-level separation.

ACKNOWLEDGMENTS

The research was headed by Project "Belanoda—Multidisciplinary graduate and post-graduate education in big data analysis for life sciences" (CPEA-LT-2016/10126), funded by the Eurasia program, SIU.

CONFLICT OF INTEREST

None declared.

AUTHOR CONTRIBUTION

Margarita Smirnova: Data curation (lead); Formal analysis (equal); Investigation (lead); Visualization (equal); Writing-original draft (lead). **Uladzislau Miamin:** Supervision (supporting). **Achim Kohler:**

Data curation (equal); Formal analysis (equal); Funding acquisition (lead); Project administration (lead); Software (lead); Writing-original draft (equal). **Leonid Valentovich:** Formal analysis (equal); Supervision (supporting); Visualization (equal); Writing-original draft (supporting). **Artur Akhremchuk:** Formal analysis (equal). **Anastasiya Sidarenka:** Supervision (supporting). **Andrey Dolgikh:** Visualization (equal). **Volha Shapaval:** Conceptualization (lead); Data curation (equal); Formal analysis (equal); Funding acquisition (lead); Methodology (lead); Project administration (lead); Writing-original draft (equal).

ETHICS STATEMENT

None required.

DATA AVAILABILITY STATEMENT

Supplemental materials containing OTU abundances per snow sample are available in Zenodo at <https://doi.org/10.5281/zenodo.4297982>. The sequence data of forty-five fast-growing bacterial isolates are available in GenBank at <https://www.ncbi.nlm.nih.gov/genbank> under accession numbers listed in Table 2. The sequence data from the green snow samples G.S.S1 and G.S.S2 are available at <https://www.ncbi.nlm.nih.gov/sra> under the accession numbers SRR12960529 and SRR12960528, respectively (BioProject PRJNA673676: <https://www.ncbi.nlm.nih.gov/bioproject/PRJNA673676>).

ORCID

Margarita Smirnova  <https://orcid.org/0000-0001-8644-8217>

REFERENCES

- Akiyama, M. (1979). *Some ecological and taxonomic observations on the colored snow algae found in Rumpa and Skarvsnes, Antarctica*. National Institute of Polar Research.
- Al-Qadiri, H. M., Lin, M., Cavinato, A. G., & Rasco, B. A. (2006). Fourier transform infrared spectroscopy, detection and identification of *Escherichia coli* O157:H7 and *Alicyclobacillus* strains in apple juice. *International Journal of Food Microbiology*, 111, 73–80.
- Altaee, N., Fahdil, A., Yousif, E., & Sudesh, K. (2016). Recovery and subsequent characterization of polyhydroxybutyrate from *Rhodococcus equi* cells grown on crude palm kernel oil. *Journal of Taibah University for Science*, 10, 543–550.
- Amamcharla, J. K., Panigrahi, S., Logue, C. M., Marchello, M., & Sherwood, J. S. (2010). Fourier transform infrared spectroscopy (FTIR) as a tool for discriminating *Salmonella typhimurium* contaminated beef. *Sensing and Instrumentation for Food Quality and Safety*, 4, 1–12.
- Amiali, N. M., Mulvey, M. R., Sedman, J., Simor, A. E., & Ismail, A. A. (2007). Epidemiological typing of methicillin-resistant *Staphylococcus aureus* strains by Fourier transform infrared spectroscopy. *Journal of Microbiological Methods*, 69, 146–153.
- Antony, R., Sanyal, A., Kapse, N., Dhakephalkar, P. K., Thamban, M., & Nair, S. (2016). Microbial communities associated with Antarctic snow pack and their biogeochemical implications. *Microbiological Research*, 192, 192–202.
- Baeza, M., Barahona, S., Alcaíno, J., & Cifuentes, V. (2017). Amplicon-metagenomic analysis of fungi from Antarctic terrestrial habitats. *Frontiers in Microbiology*, 8, 2235.
- Bajerski, F., Ganzert, L., Mangelsdorf, K., Lipski, A., & Wagner, D. (2011). *Cryobacterium arcticum* sp. nov., a psychrotolerant Bacterium

- from an Arctic soil. *International Journal of Systematic Evolutionary Microbiology*, 61, 1849–1853.
- Bockheim, J. G. (2015). *The soils of Antarctica*. Springer.
- Busse, H.-J. (2016). Review of the taxonomy of the genus *Arthrobacter*, emendation of the genus *Arthrobacter sensu lato*, proposal to re-classify selected species of the genus *Arthrobacter* in the novel genera *Glutamicibacter* gen. nov., *Paeniglutamicibacter* gen. nov., *Pseudoglutamicibacter* gen. nov., *Paenarthrobacter* gen. nov. and *Pseudarthrobacter* gen. nov., and emended description of *Arthrobacter roseus*. *International Journal of Systematic Evolutionary Microbiology*, 66, 9–37.
- Byrtusová, D., Shapaval, V., Holub, J., Šimanský, S., Rapta, M., Szotkowski, M., Kohler, A., & Márová, I. (2020). Revealing the potential of lipid and β -Glucans coproduction in *Basidiomycetes* Yeast. *Microorganisms*, 8, 1034.
- Cámara-Martos, F., Lopes, J. A., Moreno-Rojas, R., & Pérez-Rodríguez, F. (2015). Detection and quantification of *Escherichia coli* and *Pseudomonas aeruginosa* in cow milk by near-infrared spectroscopy. *International Journal of Dairy Technology*, 68, 357–365.
- Carpenter, E. J., Lin, S., & Capone, D. G. (2000). Bacterial activity in South Pole snow. *Applied and Environmental Microbiology*, 66, 4514–4517.
- Chuvochina, M., Alekhina, I., Normand, P., Petit, J.-R., & Bulat, S. (2011). Three events of Saharan dust deposition on the Mont Blanc glacier associated with different snow-colonizing bacterial phylotypes. *Microbiology*, 80, 125–131.
- Chuvochina, M. S., Marie, D., Chevaillier, S., Petit, J.-R., Normand, P., Alekhina, I. A., & Bulat, S. A. (2009). Community variability of bacteria in alpine snow (Mont Blanc) containing Saharan dust deposition and their snow colonisation potential. *Microbes Environments*, 26, 237–247.
- Colabella, C., Corte, L., Roscini, L., Shapaval, V., Kohler, A., Tafintseva, V., Tascini, C., & Cardinali, G. (2017). Merging FT-IR and NGS for simultaneous phenotypic and genotypic identification of pathogenic *Candida* species. *PLoS One*, 12, e0188104.
- Curk, M., Peledan, F., & Hubert, J. (1994). Fourier transform infrared (FTIR) spectroscopy for identifying *Lactobacillus* species. *FEMS Microbiology Letters*, 123, 241–248.
- Davey, M. P., Norman, L., Sterk, P., Huete-Ortega, M., Bunbury, F., Loh, B. K. W., Stockton, S., Peck, L. S., Convey, P., & Newsham, K. K. (2019). Snow algae communities in Antarctica: Metabolic and taxonomic composition. *New Phytologist*, 222, 1242–1255.
- Duetz, W. A., Rüedi, L., Hermann, R., O'Connor, K., Büchs, J., & Witholt, B. (2000). Methods for intense aeration, growth, storage, and replication of bacterial strains in microtiter plates. *Applied and Environmental Microbiology*, 66, 2641–2646.
- Dziewit, L., Cegielski, A., Romaniuk, K., Uhrynowski, W., Szych, A., Niesiobedzki, P., Zmuda-Baranowska, M. J., Zdanowski, M. K., & Bartosik, D. (2013). Plasmid diversity in arctic strains of *Psychrobacter* spp. *Extremophiles*, 17, 433–444.
- Dzurendova, S., Zimmermann, B., Kohler, A., Tafintseva, V., Slany, O., Certik, M., & Shapaval, V. (2020a). Microcultivation and FTIR spectroscopy-based screening revealed a nutrient-induced co-production of high-value metabolites in oleaginous *Mucoromycota* fungi. *PLoS One*, 15, e0234870.
- Dzurendova, S., Zimmermann, B., Tafintseva, V., Kohler, A., Ekeberg, D., & Shapaval, V. (2020b). The influence of phosphorus source and the nature of nitrogen substrate on the biomass production and lipid accumulation in oleaginous *Mucoromycota* fungi. *Applied Microbiology and Biotechnology*, 104, 8065–8076.
- Essendoubi, M., Toubas, D., Lepouse, C., Leon, A., Bourgeade, F., Pinon, J.-M., Manfait, M., & Sockalingum, G. D. (2007). Epidemiological investigation and typing of *Candida glabrata* clinical isolates by FTIR spectroscopy. *Journal of Microbiological Methods*, 71, 325–331.
- Fierer, N., Liu, Z., Rodríguez-Hernández, M., Knight, R., Henn, M., & Hernandez, M. T. (2008). Short-term temporal variability in airborne bacterial and fungal populations. *Applied and Environmental Microbiology*, 74, 200–207.
- Forfang, K., Zimmermann, B., Kosa, G., Kohler, A., & Shapaval, V. (2017). FTIR spectroscopy for evaluation and monitoring of lipid extraction efficiency for oleaginous fungi. *PLoS One*, 12, e0170611.
- Frey, B., Bühler, L., Schmutz, S., Zumsteg, A., & Furrer, G. (2013). Molecular characterization of phototrophic microorganisms in the forefield of a receding glacier in the Swiss Alps. *Environmental Research Letters*, 8, 15033.
- Fujii, M., Takano, Y., Kojima, H., Hoshino, T., Tanaka, R., & Fukui, M. (2010). Microbial community structure, pigment composition, and nitrogen source of red snow in Antarctica. *Microbial Ecology*, 59, 466–475.
- Gaspar, J. M. (2018). NGmerge: merging paired-end reads via novel empirically-derived models of sequencing errors. *BMC Bioinformatics*, 19, 1–9.
- Gong, C., Lai, Q., Cai, H., Jiang, Y., Liao, H., Liu, Y., & Xue, D. (2020). *Cryobacterium soli* sp. nov., isolated from forest soil. *International Journal of Systematic and Evolutionary Microbiology*, 70, 675–679.
- Gordon, R. E., Barnett, D. A., Handerman, J. E., & Pang, C. H.-N. (1974). *Nocardia coeliaca*, *Nocardia autotrophica*, and the *nocardin* strain. *International Journal of Systematic Evolutionary Microbiology*, 24, 54–63.
- Grewal, M. K., Jaiswal, P., & Jha, S. N. (2014). Detection of poultry meat specific bacteria using FTIR spectroscopy and chemometrics. *Food Science and Technology*, 52, 3859–3869.
- Guillén, M. D., Cabo, N., & Chemistry, F. (1998). Relationships between the composition of edible oils and lard and the ratio of the absorbance of specific bands of their Fourier transform infrared spectra. Role of some bands of the fingerprint region. *Journal of Agricultural*, 46, 1788–1793.
- Hanafi, M., Kohler, A., & Qannari, E.-M. (2011). Connections between multiple co-inertia analysis and consensus principal component analysis. *Chemometrics Intelligent Laboratory Systems*, 106, 37–40.
- Harding, T., Jungblut, A. D., Lovejoy, C., & Vincent, W. F. (2011). Microbes in high arctic snow and implications for the cold biosphere. *Applied and Environmental Microbiology*, 77, 3234–3243.
- Harisha, S. (2007). *Biotechnology procedures and experiments handbook (An introduction to biotechnology)*. Infinity Science Press LLC.
- Harz, M., Rösch, P., & Popp, J. (2009). Vibrational spectroscopy—A powerful tool for the rapid identification of microbial cells at the single-cell level. *Cytometry Part A: The Journal of the International Society for Analytical Cytology*, 75, 104–113.
- Hassani, S., Hanafi, M., Qannari, E. M., & Kohler, A. (2013). Deflation strategies for multi-block principal component analysis revisited. *Chemometrics Intelligent Laboratory Systems*, 120, 154–168.
- Hisakawa, N., Quistad, S. D., Hester, E. R., Martynova, D., Maughan, H., Sala, E., Gavrilov, M. V., & Rohwer, F. (2015). Metagenomic and satellite analyses of red snow in the Russian Arctic. *PeerJ*, 3, e1491.
- Hong, K., Sun, S., Tian, W., Chen, G., & Huang, W. (1999). A rapid method for detecting bacterial polyhydroxyalkanoates in intact cells by Fourier transform infrared spectroscopy. *Applied Microbiology Biotechnology*, 51, 523–526.
- Jackson, M., Mantsch, H. H., & Biology, M. (1995). The use and misuse of FTIR spectroscopy in the determination of protein structure. *Critical Reviews in Biochemistry*, 30, 95–120.
- Kageyama, A., Morisaki, K., Ōmura, S., & Takahashi, Y. (2008). *Arthrobacter oryzae* sp. nov. and *Arthrobacter humicola* sp. nov. *International Journal of Systematic Evolutionary Microbiology*, 58, 53–56.
- Kiefer, J., Ebel, N., Schlücker, E., & Leipertz, A. (2010). Characterization of *Escherichia coli* suspensions using UV/Vis/NIR absorption spectroscopy. *Analytical Methods*, 2, 123–128.
- Klassen, J. L., & Foght, J. M. (2011). Characterization of *Hymenobacter* isolates from Victoria Upper Glacier, Antarctica reveals five new

- species and substantial non-vertical evolution within this genus. *Extremophiles*, 15, 45–57.
- Klindworth, A., Pruesse, E., Schweer, T., Peplies, J., Quast, C., Horn, M., & Glöckner, F. O. (2013). Evaluation of general 16S ribosomal RNA gene PCR primers for classical and next-generation sequencing-based diversity studies. *Nucleic Acids Research*, 41, e1.
- Kohler, A., Böcker, U., Shapaval, V., Forsmark, A., Andersson, M., Warringer, J., Martens, H., Omholt, S. W., & Blomberg, A. (2015). High-throughput biochemical fingerprinting of *Saccharomyces cerevisiae* by Fourier transform infrared spectroscopy. *PLoS One*, 10, e0118052.
- Kohler, A., Kirschner, C., Oust, A., & Martens, H. (2005). Extended multiplicative signal correction as a tool for separation and characterization of physical and chemical information in Fourier transform infrared microscopy images of cryo-sections of beef loin. *Applied Spectroscopy*, 59, 707–716.
- Kohler, A., Solheim, J. H., Tafintseva, V., Zimmermann, B., & Shapaval, V. (2020). Model-based pre-processing in vibrational spectroscopy. Elsevier.
- Kojima, H., Fukuhara, H., & Fukui, M. (2009). Community structure of microorganisms associated with reddish-brown iron-rich snow. *Systematic Applied Microbiology*, 32, 429–437.
- Koller, M. (2017). Production of polyhydroxyalkanoate (PHA) biopolyesters by extremophiles. *MOJ Polymer Science*, 1, 1–19.
- Kosa, G., Kohler, A., Tafintseva, V., Zimmermann, B., Forfang, K., Afseth, N. K., Tzimiras, D., Vuoristo, K. S., Horn, S. J., & Mounier, J. (2017a). Microtiter plate cultivation of oleaginous fungi and monitoring of lipogenesis by high-throughput FTIR spectroscopy. *Microbial Cell Factories*, 16, 101.
- Kosa, G., Shapaval, V., Kohler, A., & Zimmermann, B. (2017b). FTIR spectroscopy as a unified method for simultaneous analysis of intra- and extracellular metabolites in high-throughput screening of microbial bioprocesses. *Microbial Cell Factories*, 16, 195.
- Kosa, G., Vuoristo, K. S., Horn, S. J., Zimmermann, B., Afseth, N. K., Kohler, A., & Shapaval, V. (2018a). Assessment of the scalability of a microtiter plate system for screening of oleaginous microorganisms. *Applied Microbiology Biotechnology*, 102, 4915–4925.
- Kosa, G., Zimmermann, B., Kohler, A., Ekeberg, D., Afseth, N. K., Mounier, J., & Shapaval, V. (2018b). High-throughput screening of *Mucoromycota* fungi for production of low- and high-value lipids. *Biotechnology for Biofuels*, 11, 66.
- Kumar, S., Stecher, G., Li, M., Knyaz, C., & Tamura, K. (2018). MEGA X: molecular evolutionary genetics analysis across computing platforms. *Molecular Biology and Evolution*, 35, 1547–1549.
- Lane, D. J. (1991). 16S/23S rRNA sequencing. In *Nucleic acid techniques in bacterial systematics* (pp. 115–175).
- Larose, C., Berger, S., Ferrari, C., Navarro, E., Dommergue, A., Schneider, D., & Vogel, T. M. (2010). Microbial sequences retrieved from environmental samples from seasonal Arctic snow and meltwater from Svalbard, Norway. *Extremophiles*, 14, 205–212.
- Larose, C., Dommergue, A., & Vogel, T. M. (2013). The dynamic arctic snow pack: an unexplored environment for microbial diversity and activity. *Biology*, 2, 317–330.
- Lazzaro, A., Wismer, A., Schneebeil, M., Erny, I., & Zeyer, J. (2015). Microbial abundance and community structure in a melting alpine snowpack. *Extremophiles*, 19, 631–642.
- Lee, J., Cho, A., Yang, J. Y., Woo, J., Lee, H. K., Hong, S. G., & Kim, O.-S. (2016). Complete genome sequence of *Cryobacterium arcticum* strain PAMC 27867, isolated from a sedimentary rock sample in northern Victoria Land, Antarctica. *Genome Announcements*, 4, e00885-16.
- Li, J., Shapaval, V., Kohler, A., Talintyre, R., Schmitt, J., Stone, R., Gallant, A. J., & Zeze, D. A. (2016). A modular liquid sample handling robot for high-throughput Fourier transform infrared spectroscopy. In *Advances in reconfigurable mechanisms and robots II. Mechanisms and Machine Science* (Vol. 36, pp. 769–778). Springer.
- Li, S., Xiao, X., Yin, X., & Wang, F. (2006). Bacterial community along a historic lake sediment core of Ardley Island, west Antarctica. *Extremophiles*, 10, 461–467.
- Liland, K. H., Kohler, A., & Shapaval, V. (2014). Hot PLS—a framework for hierarchically ordered taxonomic classification by partial least squares. *Chemometrics and Intelligent Laboratory Systems*, 138, 41–47.
- Lin, M., Al-Holy, M., Chang, S.-S., Huang, Y., Cavinato, A. G., Kang, D.-H., & Rasco, B. A. (2005). Rapid discrimination of *Alicyclobacillus* strains in apple juice by Fourier transform infrared spectroscopy. *International Journal of Food Microbiology*, 105, 369–376.
- Ling, H. U., & Seppelt, R. D. (1993). Snow algae of the Windmill Islands, continental Antarctica. 2. *Chloromonas rubroleosa* sp. nov. (Volvocales, Chlorophyta), an alga of red snow. *European Journal of Phycology*, 28, 77–84.
- Liu, Y., Yao, T., Jiao, N., Kang, S., Xu, B., Zeng, Y., Huang, S., & Liu, X. (2009). Bacterial diversity in the snow over Tibetan Plateau Glaciers. *Extremophiles*, 13, 411–423.
- Lohumi, S., Lee, S., Lee, H., & Cho, B.-K. (2015). A review of vibrational spectroscopic techniques for the detection of food authenticity and adulteration. *Trends in Food Science Technology*, 46, 85–98.
- Lopatina, A., Krylenkov, V., & Severinov, K. (2013). Activity and bacterial diversity of snow around Russian Antarctic stations. *Research in Microbiology*, 164, 949–958.
- Lu, J., Breitwieser, F. P., Thielen, P., & Salzberg, S. L. (2017). Bracken: estimating species abundance in metagenomics data. *PeerJ Computer Science*, 3, e104.
- Lutz, S., Anesio, A. M., Jorge Villar, S. E., & Benning, L. G. (2014). Variations of algal communities cause darkening of a Greenland glacier. *FEMS Microbiology Ecology*, 89, 402–414.
- Lutz, S., Anesio, A. M., Raiswell, R., Edwards, A., Newton, R. J., Gill, F., & Benning, L. G. (2016). The biogeography of red snow microbiomes and their role in melting arctic glaciers. *Nature Communications*, 7, 11968.
- Maccario, L., Carpenter, S. D., Deming, J. W., Vogel, T. M., & Larose, C. (2019). Sources and selection of snow-specific microbial communities in a Greenlandic sea ice snow cover. *Scientific Reports*, 9, 2290.
- Maccario, L., Sanguino, L., Vogel, T. M., & Larose, C. (2015). Snow and ice ecosystems: not so extreme. *Research in Microbiology*, 166, 782–795.
- Maccario, L., Vogel, T. M., & Larose, C. (2014). Potential drivers of microbial community structure and function in Arctic spring snow. *Frontiers in Microbiology*, 5, 413.
- Maki, T., Aoki, K., Kobayashi, F., Kakikawa, M., Tobo, Y., Matsuki, A., Hasegawa, H., & Iwasaka, Y. (2011). Characterization of halo-tolerant and oligotrophic bacterial communities in Asian desert dust (KOSA) bioaerosol accumulated in layers of snow on Mount Tateyama, Central Japan. *Aerobiologia*, 27, 277–290.
- Malard, L. A., Šabacká, M., Magiopoulos, I., Mowlem, M., Hodson, A., Tranter, M., Siegert, M. J., & Pearce, D. A. (2019). Spatial variability of Antarctic Surface Snow Bacterial Communities. *Frontiers in Microbiology*, 10, 461.
- Margesin, R., & Miteva, V. (2011). Diversity and ecology of psychrophilic microorganisms. *Research in Microbiology*, 162, 346–361.
- Margesin, R., Spröer, C., Zhang, D.-C., & Busse, H.-J. (2012). *Polaromonas glacialis* sp. nov. and *Polaromonas cryoconiti* sp. nov., isolated from alpine glacier cryoconite. *International Journal of Systematic Evolutionary Microbiology*, 62, 2662–2668.
- Marova, I., Szotkowski, M., Vanek, M., Raptá, M., Byrtusova, D., Mikheichyk, N., Haronikova, A., Certik, M., & Shapaval, V. (2017). Utilization of animal fat waste as carbon source by carotenogenic yeasts—a screening study. *The EuroBiotech Journal*, 1, 310–318.
- Meola, M., Lazzaro, A., & Zeyer, J. (2015). Bacterial composition and survival on Sahara dust particles transported to the European Alps. *Frontiers in Microbiology*, 6, 1454.
- Michaud, L., Giudice, A. L., Mysara, M., Monsieurs, P., Raffa, C., Leys, N., Amalfitano, S., & Van Houdt, R. (2014). Snow surface microbiome on the High Antarctic Plateau (DOME C). *PLoS One*, 9, e104505.
- Milius, S. (2000). Red snow, green snow. *Science News*, 157, 328–330.
- Möhler, O., Demott, P., Vali, G., & Levin, Z. (2007). Microbiology and atmospheric processes: the role of biological particles in cloud physics. *Biogeosciences*, 4(6), 1059–1071.

- Møller, A. K., Søborg, D. A., Abu Al-Soud, W., Sørensen, S. J., & Kroer, N. (2013). Bacterial community structure in High-Arctic snow and freshwater as revealed by pyrosequencing of 16S rRNA genes and cultivation. *Polar Research*, 32, 17390.
- Naumann, D. (2000). Infrared spectroscopy in microbiology. In: *Encyclopedia of analytical chemistry*.
- Novais, Â., Freitas, A. R., Rodrigues, C., & Peixe, L. (2019). Fourier transform infrared spectroscopy: unlocking fundamentals and prospects for bacterial strain typing. *European Journal of Clinical Microbiology & Infectious Diseases*, 38, 427–448.
- Pindi, P. K., Kishore, K. H., Reddy, G., & Shivaji, S. (2009). Description of *Leifsonia kafniensis* sp. nov. and *Leifsonia antarctica* sp. nov. *International Journal of Systematic Evolutionary Microbiology*, 59, 1348–1352.
- Pindi, P. K., Manorama, R., Begum, Z., & Shivaji, S. (2010). *Arthrobacter antarcticus* sp. nov., isolated from an Antarctic marine sediment. *International Journal of Systematic Evolutionary Microbiology*, 60, 2263–2266.
- Quast, C., Pruesse, E., Yilmaz, P., Gerken, J., Schweer, T., Yarza, P., Peplies, J., & Glöckner, F. O. (2012). The SILVA ribosomal RNA gene database project: Improved data processing and web-based tools. *Nucleic Acids Research*, 41, D590–D596.
- Rainey, F. A. (2011). How to describe new species of prokaryotes. In *Methods in microbiology* (Vol. 38, pp. 7–14). Elsevier.
- Reddy, G., Prakash, J., Srinivas, R., Matsumoto, G., & Shivaji, S. (2003). *Leifsonia rubra* sp. nov. and *Leifsonia aurea* sp. nov., psychrophiles from a pond in Antarctica. *International Journal of Systematic Evolutionary Microbiology*, 53, 977–984.
- Roggo, Y., Chalus, P., Maurer, L., Lema-Martinez, C., Edmond, A., & Jent, N. (2007). A review of near infrared spectroscopy and chemometrics in pharmaceutical technologies. *Journal of Pharmaceutical Biomedical Analysis*, 44, 683–700.
- Romaniuk, K., Golec, P., & Dziewit, L. (2018). Insight into the diversity and possible role of plasmids in the adaptation of psychrotolerant and metalotolerant *Arthrobacter* spp. to extreme Antarctic environments. *Frontiers in Microbiology*, 9, 3144.
- Savitzky, A., & Golay, M. J. (1964). Smoothing and differentiation of data by simplified least squares procedures. *Analytical Chemistry*, 36, 1627–1639.
- Shapaval, V., Afseth, N. K., Vogt, G., & Kohler, A. (2014). Fourier transform infrared spectroscopy for the prediction of fatty acid profiles in *Mucor* fungi grown in media with different carbon sources. *Microbial Cell Factories*, 13, 86.
- Shapaval, V., Brandenburg, J., Blomqvist, J., Tafintseva, V., Passoth, V., Sandgren, M., & Kohler, A. (2019). Biochemical profiling, prediction of total lipid content and fatty acid profile in oleaginous yeasts by FTIR spectroscopy. *Biotechnology for Biofuels*, 12, 140.
- Shapaval, V., Møretrø, T., Suso, H. P., Åsli, A. W., Schmitt, J., Lillehaug, D., Martens, H., Böcker, U., & Kohler, A. (2010). A high-throughput microcultivation protocol for FTIR spectroscopic characterization and identification of fungi. *Journal of Biophotonics*, 3, 512–521.
- Shapaval, V., Møretrø, T., Wold Åsli, A., Suso, H.-P., Schmitt, J., Lillehaug, D., & Kohler, A. (2017). A novel library-independent approach based on high-throughput cultivation in Bioscreen and fingerprinting by FTIR spectroscopy for microbial source tracking in food industry. *Letters in Applied Microbiology*, 64, 335–342.
- Shapaval, V., Schmitt, J., Møretrø, T., Suso, H., Skaar, I., Åsli, A., Lillehaug, D., & Kohler, A. (2013). Characterization of food spoilage fungi by FTIR spectroscopy. *Applied Microbiology*, 114, 788–796.
- Shapaval, V., Walczak, B., Gognies, S., Møretrø, T., Suso, H., Åsli, A. W., Belarbi, A., & Kohler, A. (2012). FTIR spectroscopic characterization of differently cultivated food related yeasts. *Analyst*, 138, 4129–4138.
- Shivaji, S., Reddy, G., Raghavan, P., Sarita, N., & Delille, D. (2004). *Psychrobacter salsus* sp. nov. and *Psychrobacter adeliensis* sp. nov. isolated from fast ice from Adelie Land, Antarctica. *Systematic Applied Microbiology*, 27, 628–635.
- Sjöling, S., & Cowan, D. A. (2003). High 16S rDNA bacterial diversity in glacial meltwater lake sediment, Bratina Island, Antarctica. *Extremophiles*, 7, 275–282.
- Tafintseva, V., Shapaval, V., Smirnova, M., & Kohler, A. (2020). Extended multiplicative signal correction for FTIR spectral quality test and pre-processing of infrared imaging data. *Journal of Biophotonics*, 13, e201960112.
- Tamura, K., & Nei, M. (1993). Estimation of the number of nucleotide substitutions in the control region of mitochondrial DNA in humans and chimpanzees. *Molecular Biology and Evolution*, 10, 512–526.
- Terashima, M., Umezawa, K., Mori, S., Kojima, H., & Fukui, M. (2017). Microbial community analysis of colored snow from an alpine snowfield in northern Japan reveals the prevalence of Betaproteobacteria with snow algae. *Frontiers in Microbiology*, 8, 1481.
- Thomas, W. H., & Duval, B. (1995). Sierra Nevada, California, U.S.A., Snow Algae: Snow Albedo Changes, Algal-Bacterial Interrelationships, and Ultraviolet Radiation Effects. *Arctic and Alpine Research*, 27, 389–399.
- van de Voort, F. (1992). Fourier transform infrared spectroscopy applied to food analysis. *Food Research International*, 25, 397–403.
- Wang, F., Gai, Y., Chen, M., & Xiao, X. (2009). *Arthrobacter psychrochitiniphilus* sp. nov., a psychrotrophic bacterium isolated from Antarctica. *International Journal of Systematic Evolutionary Microbiology*, 59, 2759–2762.
- Whipps, J. M. (2001). Microbial interactions and biocontrol in the rhizosphere. *Journal of Experimental Botany*, 52, 487–511.
- Wood, D. E., Lu, J., & Langmead, B. (2019). Improved metagenomic analysis with Kraken 2. *Genome Biology*, 20, 257.
- Wunderlin, T., Ferrari, B., & Power, M. (2016). S. *FEMS Microbiology Ecology*, 92, fiw132.
- Xiong, Y., Shapaval, V., Kohler, A., & From, P. J. (2019a). A laboratory-built fully automated ultrasonication robot for filamentous fungi homogenization. *SLAS Technology: Translating Life Sciences Innovation*, 24, 583–595.
- Xiong, Y., Shapaval, V., Kohler, A., Li, J., & From, P. J. (2019b). A fully automated robot for the preparation of fungal samples for FTIR spectroscopy using deep learning. *IEEE Access*, 7, 132763–132774.
- Yoon, S.-H., Ha, S.-M., Kwon, S., Lim, J., Kim, Y., Seo, H., & Chun, J. (2017). Introducing EzBioCloud: A taxonomically united database of 16S rRNA gene sequences and whole-genome assemblies. *International Journal of Systematic and Evolutionary Microbiology*, 67, 1613.
- Zeng, Y.-X., Yan, M., Yu, Y., Li, H.-R., He, J.-F., Sun, K., & Zhang, F. (2013). Diversity of bacteria in surface ice of Austre Lovénbreen glacier, Svalbard. *Archives of Microbiology*, 195, 313–322.
- Zhang, S., Yang, G., Wang, Y., & Hou, S. (2010). Abundance and community of snow bacteria from three glaciers in the Tibetan Plateau. *Journal of Environmental Sciences*, 22, 1418–1424.
- Zhang, Y.-Q., Li, W.-J., Kroppenstedt, R. M., Kim, C.-J., Chen, G.-Z., Park, D.-J., Xu, L.-H., & Jiang, C.-L. (2005). *Rhodococcus yunnanensis* sp. nov., a mesophilic actinobacterium isolated from forest soil. *International Journal of Systematic Evolutionary Microbiology*, 55, 1133–1137.
- Zimmermann, B., & Kohler, A. (2013). Optimizing Savitzky-Golay parameters for improving spectral resolution and quantification in infrared spectroscopy. *Applied Spectroscopy*, 67, 892–902.

How to cite this article: Smirnova M, Miamin U, Kohler A, et al. Isolation and characterization of fast-growing green snow bacteria from coastal East Antarctica. *MicrobiologyOpen*. 2021;10:e1152. <https://doi.org/10.1002/mbo3.1152>

APPENDIX A

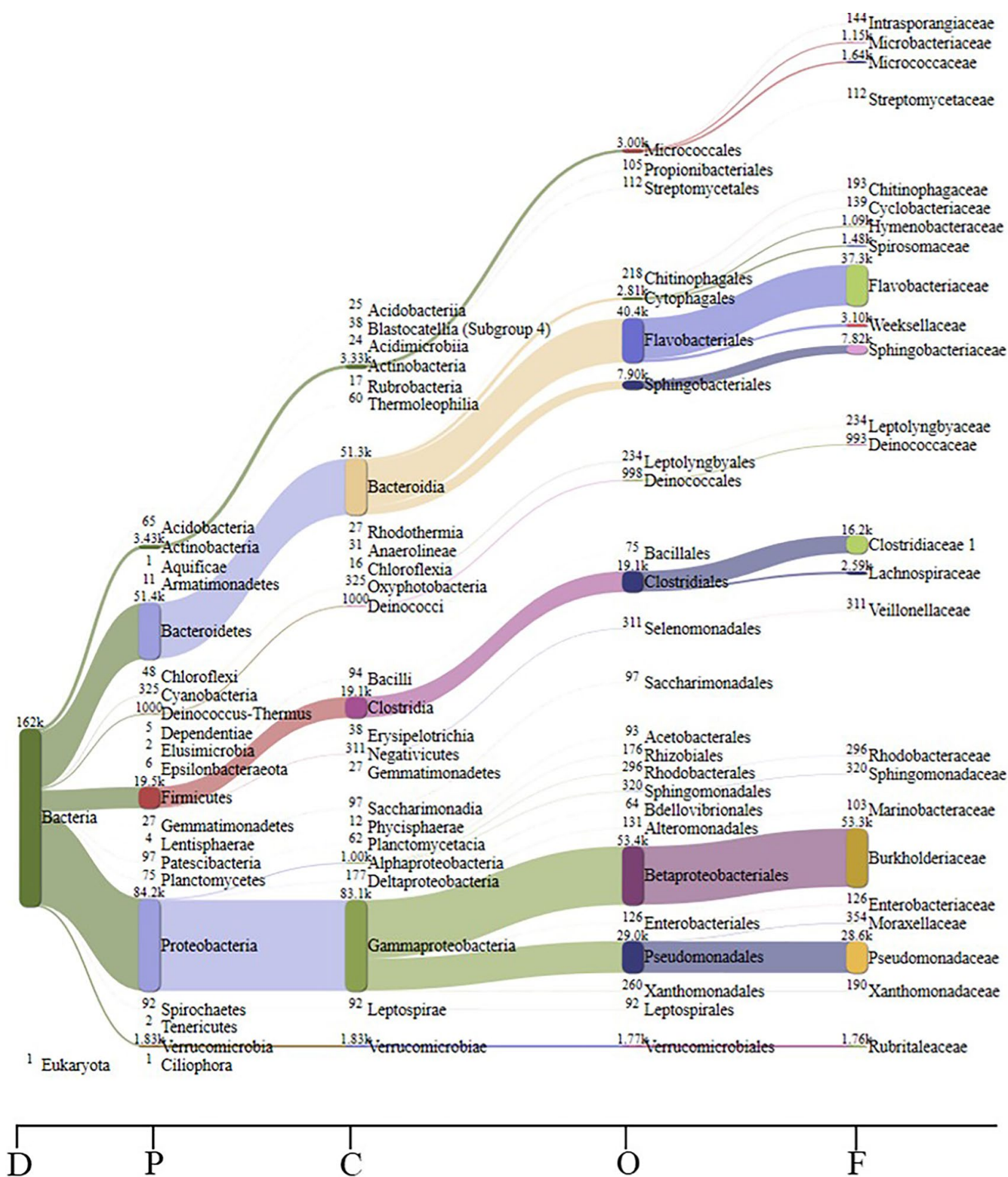


FIGURE A1 Visualization of metagenome results of green snow sample 1 (G.S.S1), where D—domain, P—phylum, O—order, F—family

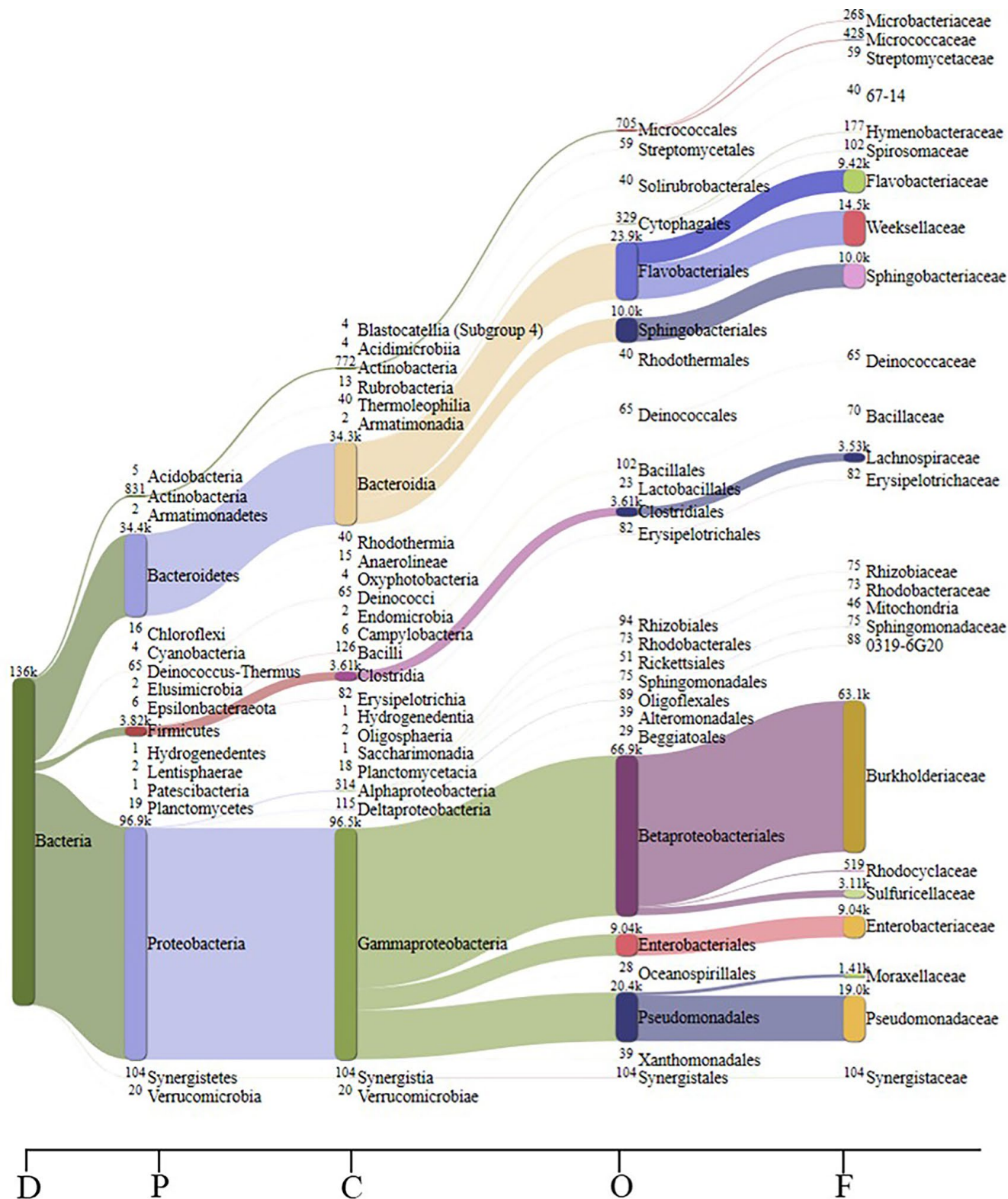


FIGURE A2 Visualization of metagenome results of green snow sample 2 (G.S.S2), where D—domain, P—phylum, O—order, F—family

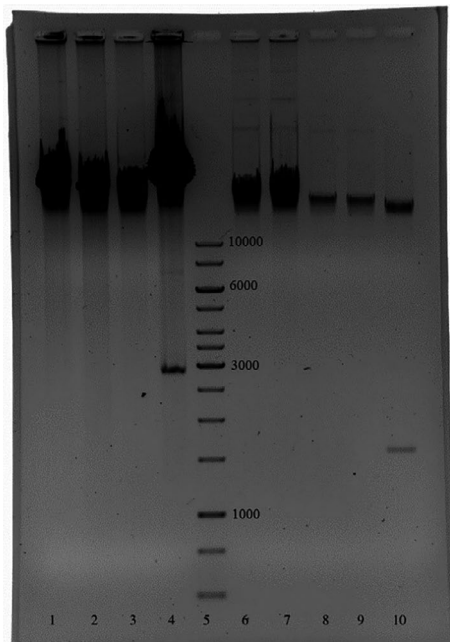


FIGURE A3 Electrophoresis image of total DNA:
 1—*Arthrobacter* sp. G.S.37, 2—*Arthrobacter* sp. G.S.7, 3—*Arthrobacter* sp. G.S.29, 4—*Psychrobacter glacinicola* G.S.11, 5—GeneRuler 1 kb DNA Ladder, 6—*Cryobacterium soli* G.S.39, 7—*Cryobacterium soli* G.S.40, 8—*Cryobacterium soli* G.S.2, 9—*Cryobacterium arcticum* G.S.1, 10—*Escherichia coli* XL1-Blue [pUC18]

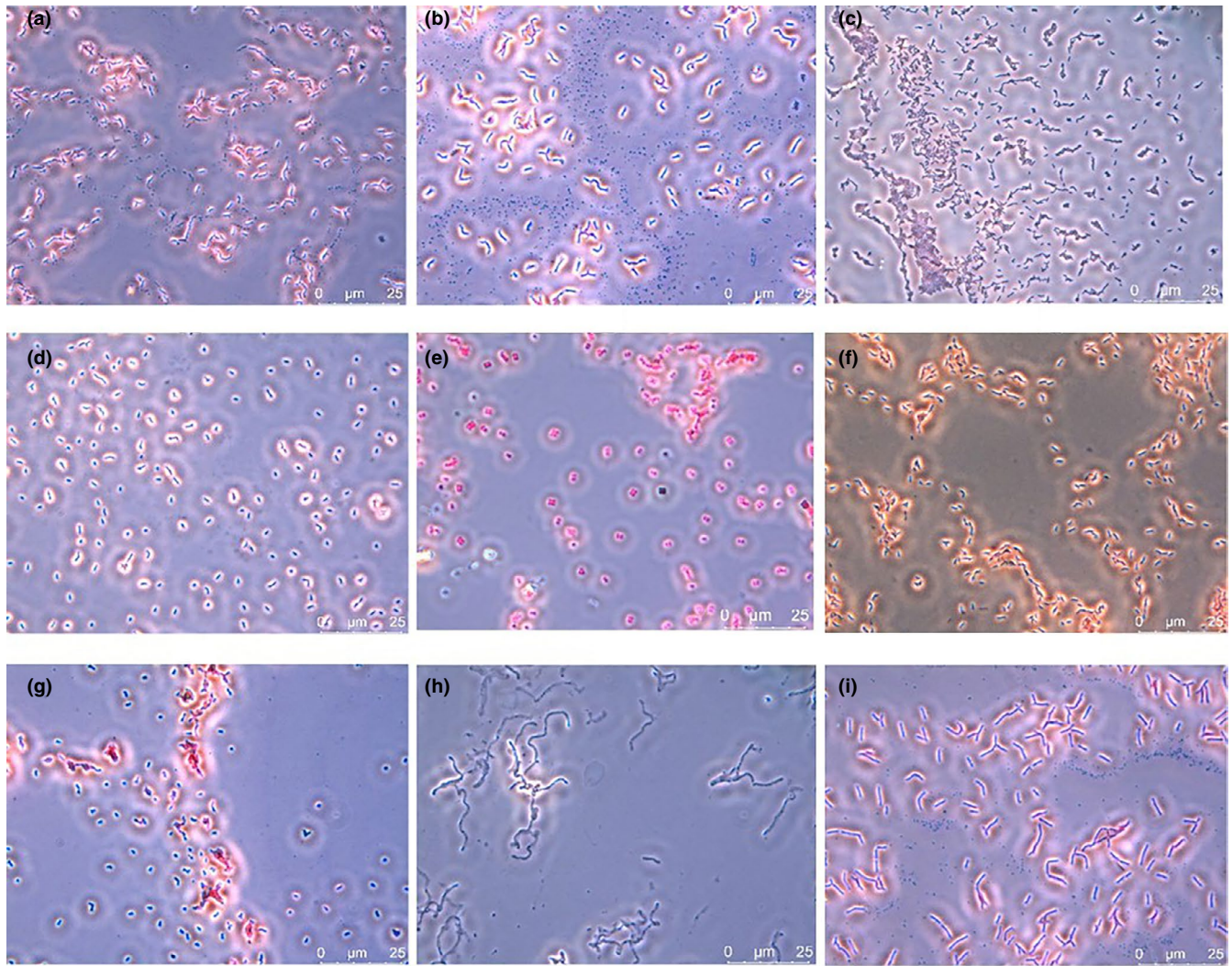


FIGURE A4 Cell morphology of the Gram-stained Antarctic green snow fast-growing bacteria: (a) *Cryobacterium arcticum* G.S.1; (b) *Rhodococcus yunnanensis* G.S.3; (c) *Leifsonia antarctica* G.S.13; (d) *Arthrobacter* sp. G.S.29; (e) *Psychrobacter glacinicola* G.S.11; (f) *Pseudomonas fluorescens* G.S.33; (g) *Paeniglutamicibacter antarcticus* G.S.38; (h) *Polaromonas* sp. G.S.42; (i) *Rhodococcus erythropolis* G.S.44

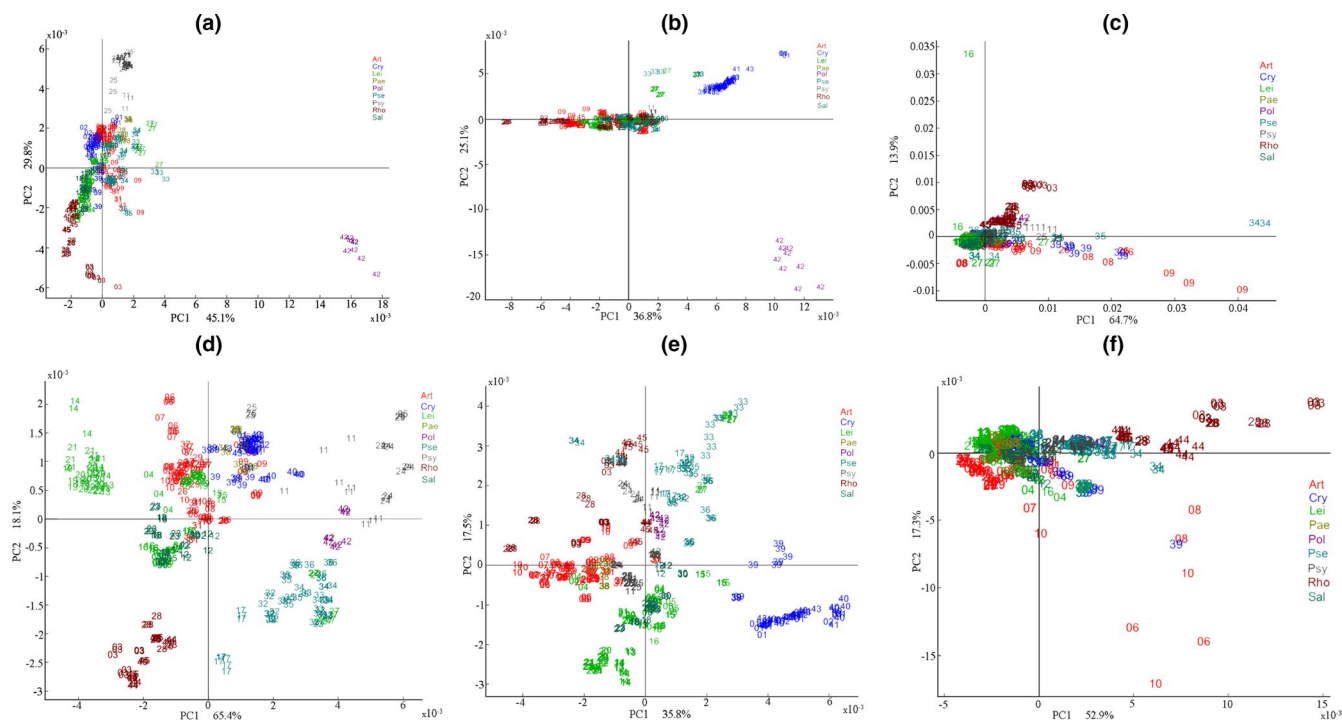


FIGURE A5 PCA scatter plots of lipid/ester/PHA (a and d), polysaccharide (b and e), and protein (c and f) regions of FTIR spectra of Antarctic green snow bacteria cultivated on BHI agar (a, b and c) and BHI broth (d, e, and f). The numbers on PCA plots indicate samples and are related to the isolate number in the G.S. abbreviation (Table 2). The colors of samples on PCA plots are corresponding to the genus abbreviations: Art—*Arthrobacter*; Cry—*Cryobacterium*; Lei—*Leifsonia*; Pae—*Paeniglutamicibacter*; Pol—*Polaromonas*; Pse—*Pseudomonas*; Psy—*Psychrobacter*; Rho—*Rhodococcus*; Sal—*Salinibacterium*

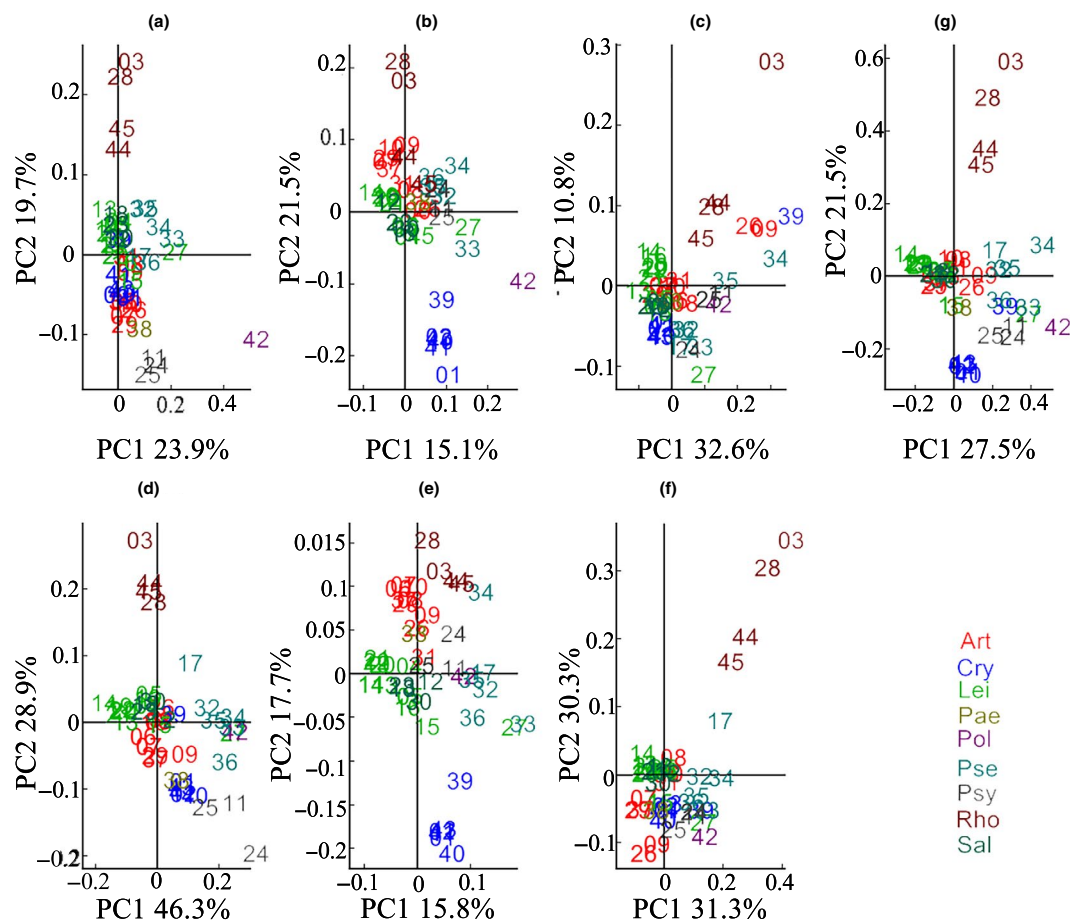


FIGURE A6 Multiblock PCA scatter plots of lipid/ester/PHA (a and d), polysaccharide (b and e), and protein (c and f) regions of FTIR-HTS spectra of Antarctic green snow bacteria cultivated on BHI agar (a, b, and c) and BHI broth (d, e, and f). Multiblock PCA consensus is presented on (g). The numbers on PCA plots indicate samples and are related to the isolate number in G.S. abbreviation (Table 2). The colors of samples on PCA plots are corresponding to the genus abbreviations: Art—*Arthrobacter*; Cry—*Cryobacterium*; Lei—*Leifsonia*; Pae—*Paeniglutamicibacter*; Pol—*Polaromonas*; Pse—*Pseudomonas*; Psy—*Psychrobacter*; Rho—*Rhodococcus*; Sal—*Salinibacterium*